THE JOURNAL OF BIOLOGICAL CHEMISTRY VOL. 281, NO. 38, pp. 28113–28121, September 22, 2006

Ets-1-dependent Expression of Vascular Endothelial Growth Factor Receptors Is Activated by Latency-associated Nuclear Antigen of Kaposi's Sarcoma-associated Herpesvirus through Interaction with Daxx*

Received for publication, March 3, 2006, and in revised form, July 19, 2006 Published, JBC Papers in Press, July 20, 2006, DOI 10.1074/jbc.M602026200

Yuko Murakami[‡], Satoshi Yamagoe[‡1], Kohji Noguchi[‡], Yutaka Takebe[§], Naoko Takahashi[‡], Yoshimasa Uehara[‡], and Hidesuke Fukazawa[‡]

From the [‡]Department of Bioactive Molecules and [§]Laboratory of Molecular Virology and Epidemiology, AIDS Research Center, National Institute of Infectious Diseases, Tokyo 162, Japan

Vascular endothelial growth factor (VEGF) and its receptors are highly expressed in Kaposi's sarcoma (KS) lesion and play a key role in angiogenesis. Latency-associated nuclear antigen (LANA) of Kaposi's sarcoma-associated herpesvirus (KSHV/HHV8) has multiple functions related to viral latency and KSHV-induced oncogenesis. In this report, we have identified Daxx as a LANA-binding protein by co-immunoprecipitation analysis of HeLa cells stably expressing LANA. LANA associated with Daxx in a PEL cell line infected with KSHV. LANA and Daxx also bound *in vitro*, suggesting direct interaction. From the results of binding assays, a region containing the Glu/Asp-rich domain within LANA, and a central region including the second paired amphipathic helix within Daxx contributed to the interaction. To address the physiological significance of this interaction, we focused on a Daxx-mediated VEGF receptor gene regulation. We found that Daxx repressed Ets-1-dependent Flt-1/VEGF receptor-1 gene expression, and that LANA inhibited the repression by Daxx in a reporter assay. Analyses of flow cytometry and real-time PCR revealed that expression of VEGF receptor-1 and -2 in LANA-expressing human umbilical vein endothelial cells (HUVECs) significantly increased. Co-immunoprecipitation and immunoblotting experiments suggested that LANA-bound Daxx to inhibit the interaction between Daxx and Ets-1. Chromatin immunoprecipitation assays showed that Daxx associated with VEGF receptor-1 promoter in HUVECs, and that LANA expression reduced this association. These results suggested that LANA contributes to a high expression of VEGF receptors in KS lesion by interfering with the interaction between Daxx and Ets-1.

Kaposi's sarcoma-associated herpesvirus (KSHV[2]/HHV8) has been found to be the pathogen of Kaposi's sarcoma (KS) (1) (2), two B cell malignancies, primary effusion lymphoma (PEL), and multicentric Castleman's disease (MCD) (3). Among over 80 ORFs of KSHV (4), LANA (latency-associated nuclear antigen) is exceptionally highly expressed in KS lesion, PEL, and also in MCD (5) (3), so that LANA is used as a diagnostic marker of KSHV. LANA is reported to be a multifunctional protein that tethers its own viral episomal DNA to host chromosomes in mitosis to segregate KSHV into progeny cells (6) (7) and also binds many host molecules to regulate expression of cellular genes. LANA inhibits p53-induced apoptosis (8), transforms fibroblast by co-transfection with the Ras oncogene (9) and also stabilizes β-catenin to stimulate entry into S phase (10). LANA seems to contribute to pathogenesis of KSHV-associated malignancies through these interactions.

We identified Daxx as a new LANA-interacting host protein. To know the biological significance of the interaction between LANA and Daxx, we focused on Daxx-modulated transcription. Daxx was found initially as a Fas-binding protein to regulate apoptosis (11) and later reported to bind with several nuclear proteins and transcription factors. Daxx was shown to act as a transcriptional repressor of Ets-1 (12), Pax3 (13), Pax5 (14), and p53 (15) through protein-protein interaction. In the case of Ets-1, Daxx repressed Ets-1-dependent expression of matrix metalloproteinase 1 (MMP1) and Bcl-2 (12). Ets-1 belongs to the Ets family of transcriptional factors, and regulates various gene expressions through binding to a unique motif (GGAA) on their promoters. Ets-1 regulates genes related to angiogenesis: Flt-1/VEGF receptor-1, KDR/VEGF receptor-2, and matrix metalloproteinases (MMPs) (16). Ets-1 is specifically expressed in lymphoid tissues, endothelial cells (17), and also in the spindle cells of KS lesion, derived from endothelial origins (18). In KS lesion, angiogenic factors such as VEGF and VEGF receptors were highly expressed (1) (19). Vascular angiogenesis plays an important role in the development and progression of tumors, especially KS (20) (21) (22). We therefore examined the role of LANA in interaction between Daxx

* This work was supported in part by a grant for Research on Health Sciences focusing on Drug Innovation from The Japan Human Sciences Foundation. The costs of publication of this article were defrayed in part by the payment of page charges. This article must therefore be hereby marked "*advertisement*" in accordance with 18 U.S.C. Section 1734 solely to indicate this fact.

[1] To whom correspondence should be addressed: Dept. of Bioactive Molecules, National Institute of Infectious Diseases, Toyama 1-23-1, Shinjuku-ku, Tokyo, 162–8640, Japan. Tel.: 81-3-5285-1111; Fax: 81-3-5285-1272; E-mail: syamagoe@nih.go.jp.

[2] The abbreviations used are: KSHV, Kaposi's sarcoma-associated herpesvirus; VEGF, vascular endothelial growth factor; ORF, open reading frame; DTT, dithiothreitol; PMSF, phenylmethylsulfonyl fluoride; HA, hemagglutinin; GST, glutathione *S*-transferase; DAPI, 4′,6-diamidino-2-phenylindole; ChIP, chromatin immunoprecipitation assay; GFP, green fluorescent protein; PAH, paired amphipathic helix; HUVEC, human vascular endothelial cells; LANA, latency-associated nuclear antigen; aa, amino acids; Ets, E26 transformation-specific.

and Ets-1, and show here a possible new function of LANA on the expression of VEGF receptors.

EXPERIMENTAL PROCEDURES

Plasmids—LANA gene was cut from L54 Lambda FIX II vector (NIH AIDS Research & Reference Reagent Program), at the EheI site (123743 and 127293 of KSU75698) and inserted into the EcoRV site of pFLAG-CMV-2 expression vector (Sigma) to make an N-terminal FLAG-tagged LANA expression vector, pFLAG-LANA. For *in vitro* translation/transcription system, the *LANA* gene from pFLAG-LANA was subcloned between the EcoRI and KpnI sites of pBluescript II KS(+) plasmid after correction of the N-terminal 5 bases using synthetic oligonucleotides, 5′-AATTCATCGATGGCGCCCCCGGGA-ATGCG-3′ and 5′-CATTCCCGGGGGCTCTATCGATG-3′ (using EcoRI and BsmI sites), to obtain pBluescript-LANA. A series of C-terminal deletion mutants of LANA (L1 to L4) were constructed from pBluescript-LANA using an exonuclease III/mung bean deletion kit (Toyobo, Tokyo, Japan) according to the manufacturer's instructions. An N-terminal deletion mutant of LANA (L5) was constructed with pBluescript-LANA by cutting the N-terminal region at EcoRI and PstI sites and joining it with synthetic oligonucleotides, 5′-AATTCATC-GATGGAGCCCCTGCA-3′ and 5′-GGGCTCCATCGATG-3′. PFLAG-LANA deletion mutants (pFLAG-LANA-N1 to pFLAG-LANA-C) were constructed with L1–L5 and pFLAG-CMV-2 vector. Full-length and various deletion mutants of the *Daxx* gene were generated by PCR amplification from cDNA of HeLa cells, subcloned into pCR-Blunt II-TOPO plasmid (Invitrogen, Carlsbad, CA), and cloned between the EcoRI and the SalI sites of pcDNA3.1 (−) (Invitrogen) (termed pcDNA-Daxx), pCMV-HA (Clontech Laboratories, Inc. Palo Alto, CA), or pGEX-6P-3 (Amersham Biosciences, Piscataway, NJ). A luciferase reporter plasmid, pFlt-1-luc (containing human Flt-1 promoter −748/+248, D64016) was kindly provided by Dr. K. Morishita (23). Human *ets-1* genes of p51Ets-1 and p42Ets-1 (the full-length Ets-1 and a variant lacking the regulatory domain, exon VII, respectively (24)), were cut from plasmids kindly provided by Dr. R. Li (12), and cloned into pcDNA3.1(+) (Invitrogen). The constructed plasmids were termed pcDNA-p51Ets-1 and pcDNA-p42Ets-1, respectively. For flow cytometric analysis, the full-length *LANA* gene from the pBluescript-LANA was cloned between the SacI and SalI sites of pIRES2-EGFP vector (Clontech), termed pIRES2-LANA-EGFP.

Cell Culture and Transfection—HeLa cells and human embryonic kidney 293T cells were cultured in Dulbecco's modified medium supplemented with 10% bovine fetal serum. A KSHV-infected PEL cell line, BCBL-1 cells (kindly provided by Dr. H. Katano) were cultured in RPMI 1640 with 10% bovine fetal serum. Human umbilical vein endothelial cells (HUVEC) (Clonetics, San Diego, CA) were cultured in EGM-2 medium (Clonetics). Transfection was performed with FuGENE6 (Roche Diagnostics, Indianapolis, IN) for HeLa and 293T cells or by Nucleofecter system (amaxa GmbH, Cologne, Germany) for HUVEC.

Identification of LANA-binding Protein—PFLAG-LANA was transfected into HeLa cells and stable LANA-expressing clones were selected. LANA-expressing cells of six liters were harvested, nuclear extract was prepared as previously described (25), and dialyzed against a buffer containing 20 mM Tris-HCl, pH 7.5, 100 mM NaCl, 0.2 mM EDTA, 10% glycerol, 1 mM phenylmethylsulfonyl fluoride (PMSF), and 10 mM β-mercaptoethanol. The nuclear extract was adjusted to 150 mM NaCl and 0.1% Tween 20 before absorption into anti-FLAG antibody (M2) affinity gel (Sigma). The gel was washed with 150 mM washing buffer (20 mM Tris-HCl, pH 8.0, 5 mM $MgCl_2$, 150 mM NaCl, 1 mM dithiothreitol (DTT), 10% glycerol, 1 mM PMSF), and eluted with the same buffer containing 200 μg/ml of FLAG peptides. The eluted protein was applied to SDS-PAGE and stained with Coomassie Brilliant Blue or silver stained. The Coomassie-stained band was cut and treated with lysyl endopeptidase. The extracted peptides were purified using HPLC, and analyzed with a Procise 494 HT Protein Sequencing System (Applied Biosystems, Foster City, CA).

Immunoprecipitation and Western Blotting—Cells were harvested and lysed with low salt buffer (10 mM HEPES, pH 7.9, 10 mM KCl, 1.5 mM $MgCl_2$, 1 mM DTT containing 0.5% Nonidet P-40, 1 mM PMSF, 25 μg/ml each of antipain, pepstatin, and leupeptin), then centrifuged to collect the nuclei. The nuclear pellet was lysed with nuclear extract buffer (20 mM Tris-HCl, pH 7.9, 5 mM, EDTA, 300 mM NaCl, 1 mM PMSF), and the same volume of distilled water was added. Nuclear extract was subjected to immunoprecipitation either with anti-FLAG antibody (M2), anti-Daxx antibody (sc-7152) (Santa Cruz Biotechnology, Inc., Santa Cruz, CA), or anti-Ets-1 antibody (Santa Cruz Biotechnology, sc-350). The immune complex was washed with 150 mM washing buffer, resolved in Laemmli's sample buffer and applied to SDS-PAGE. Proteins in gels were transferred to PVDF membrane followed by Western blotting using anti-FLAG antibody (M5, Sigma), anti-Daxx antibody (sc-7152), anti-LANA antibody (Advanced Biotechnologies, Columbia, MD), anti-Ets-1 antibody (sc-350), or anti-HA antibody (Sigma).

GST Pull-down Assay—Glutathione *S*-transferase (GST)-Daxx fusion proteins were expressed in *Escherichia coli*, and purified using affinity matrix glutathione-Sepharose beads (Amersham Biosciences). ^{35}S-labeled LANA was made *in vitro* with TnT quick-coupled reticulocyte transcription/translation systems (Promega, Madison, WI). GST-Daxx fusion proteins were bound to glutathione-Sepharose beads and incubated with the translated products containing ^{35}S-labeled LANA in binding buffer (25 mM HEPES, pH 7.6, 50 mM NaCl, 2.5 mM $MgCl_2$, 1 mM DTT, 0.05% Triton X-100, 1 mM PMSF) at room temperature for 15 min. After washing with washing buffer (25 mM HEPES, pH 7.6, 150 mM NaCl, 2.5 mM $MgCl_2$, 1 mM DTT, 0.5% Triton X-100, 1 mM PMSF), proteins adsorbed to the beads were resolved and applied to SDS-PAGE. Proteins in the gel were stained with Coomassie Brilliant Blue, and the radioactivity was detected by BAS-1500 (Fuji Film, Tokyo).

Immunofluorescence Assay—BCBL-1 cells were attached to slide glasses with a cell concentrator (StatSpin, Norwood, MA). HeLa cells were seeded on chamber slides (Lab-Tek, Campbell, CA). The cells were fixed in 4% paraformaldehyde in PBS(−), permeabilized with 0.2% Triton X-100, and incubated with anti-LANA antibody (Advanced Biotechnologies) (diluted to 1:500 or 1:1000) and anti-Daxx antibody (sc-7152) (diluted to

1:100 or 1:200) followed by fluorescent-conjugated second antibody (Alexa Fluor 488 anti-rat IgG and Alexa Fluor 594 anti-rabbit IgG, Molecular Probes, Eugene, OR) (diluted to 1:200 each). Cell nuclei were stained with DAPI in mounting oil (Vectashield with DAPI, Vector Laboratories, Burlingame, CA). Immunostained cells were analyzed by a confocal laser scanning microscope using a Carl Zeiss LSM510 system (Carl Zeiss, Oberkochen, Germany).

Transcriptional Reporter Assay—293T cells (2×10^5 cells/well) grown in 24-well plates were transfected with pFlt-1-luc, pRSV-β-Gal (for transfection efficiency), and the combination of pcDNA-p51Ets-1, pcDNA-p42Ets-1, pcDNA-Daxx, or pFLAG-LANA, with 2 μl of FuGENE6. Total DNA was adjusted to a constant amount (800 ng). Two days after transfection, the cells were lysed and applied to luciferase assay (Toyo Inki, Tokyo) and β-galactosidase enzyme assay system (Promega). Assays were performed in triplicate, and the experiments were repeated three times.

Flow Cytometric Analysis—HUVECs transfected with either pIRES2-LANA-EGFP or pIREAS2-EGFP as control, were subjected to FACS Vantage (Becton Dickinson, Franklin Lakes, NJ) to collect GFP-expressing cells 2 days after transfection. The GFP-expressing cells cultured for 10 days were incubated with anti-Flt-1 or anti-KDR antibody (V4262, V9134, respectively, Sigma) and PE-labeled secondary antibody (R0439, Dako Cytomation, Carpinteria, CA). The cells were analyzed by a FACS Calibur flow cytometer (Becton Dickinson).

Quantitative Real-time RT-PCR—HUVECs were transfected with either pIRES2-LANA-EGFP or pIREAS2-EGFP using Nucleofector system, and sorted with FACS Aria (Becton Dickinson) to collect GFP-expressing cells. Total RNA was extracted with RNeasy Mini kit (Qiagen GmbH, Hilden, Germany), and reverse-transcribed to cDNA with oligo(dT) by Superscript First-strand synthesis system according to the manufacturer's instructions (Invitrogen). The cDNA was applied to Real-Time PCR using SYBR Premix Ex Taq (Takara Bio Co.) with ABI PRISM7000 (Applied Biosystems). PCR was performed at 95 °C for 10 s, followed by 40 cycles of 95 °C for 5 s and 60 °C for 34 s. The primers were designed using software Primer Express (Applied Biosystems). The forward and reverse primers for Flt-1 were 5′-CCCTTATGATGCCAGCAAGTG-3′ and 5′-CCAAAAGCCCCTCTTCCAA-3′, respectively, and primers for KDR were 5′-CACCACTCAAACGCTGACATGTA-3′ and 5′-CCAACTGCCAATACCAGTGGAT-3′. Primers for Daxx were 5′-GCCCTTCACCACTGTCTTAGAGA-3′ and 5′-GAGACGCCTCCATTGAAGGA-3′. As an internal control, glyceraldehyde-3-phosphate dehydrogenase (GAPDH) was used with primers 5′-GGAGTCAACGGATTTGGTCGTA-3′, and 5′-GGCAACAATATCCACTTTACCAGAGT-3′. The primers for Ets-1 were 5′-CTGCGCCCTGGGTAAAGA-3′ and 5′-CCCATAAGATGTCCCCAACAA-3′. In the case of Ets-1, primers for GAPDH were 5′-CCACCCATGGCAAATTCC-3′ and 5′-TGGGATTTCCATTGATGACAAG-3′. Obtained data were analyzed according to the sequence detector program (Applied Biosystems).

Chromatin Immunoprecipitation (ChIP) Assay—ChIP assays were performed basically using a kit from Upstate Biotechnology (Lake Placid, NY) with some modifications. Cells (5×10^6 cells/assay) were treated with 1% formaldehyde for 5 min for cross-linking, lysed with 400 μl of lysis buffer (10 mM HEPES, pH 7.9, 60 mM KCl, 0.5% Nonidet P-40, 1 mM PMSF, 25 μg/ml each of antipain, pepstatin, and leupeptin), and centrifuged to collect the nuclei. The nuclear pellet was lysed with 200 μl of SDS lysis buffer (50 mM Tris-Hcl, pH 8.1, 10 mM EDTA, 1% SDS), and sonicated 6 times for 30 s each time. Centrifuged supernatants were then diluted with 1.8 ml of ChIP dilution buffer (0.01% SDS, 1.1% Triton X-100, 1.2 mM EDTA, 16.7 mM Tris-HCl, pH 8.0), and precleared with protein A agarose/salmon sperm DNA. Anti-Ets-1 (Santa Cruz Biotechnology, sc-350), anti-Daxx antibody (Santa Cruz Biotechnology, sc-7152), or rabbit IgG (Sigma) as the negative control was added respectively to the supernatant, and rotated overnight at 4 °C. The mixture was then incubated with protein A-agarose/salmon sperm DNA for 1 h at 4 °C. The protein A-agarose-conjugated complex was washed, and DNA fragments were eluted and prepared according to the manufacturer's instructions. The prepared DNA was resolved in 20 μl of H_2O and 2 μl was used for PCR. Primers used were 5′-GGGACCCCTTGACGTCACCA-3′ (corresponding to −90 to −71 of Flt-1 promoter) and 5′-ACCTCGATGAAGAGCAGCCG-3′ (corresponding to −12 to +8 of Flt-1 promoter). Ex Taq polymerase (Takara Bio Co.) was used, and PCR conditions were 30 cycles of 94 °C for 30 s, 55 °C for 30 s and 72 °C for 30 s. The PCR products were analyzed on a 1.8% agarose gel.

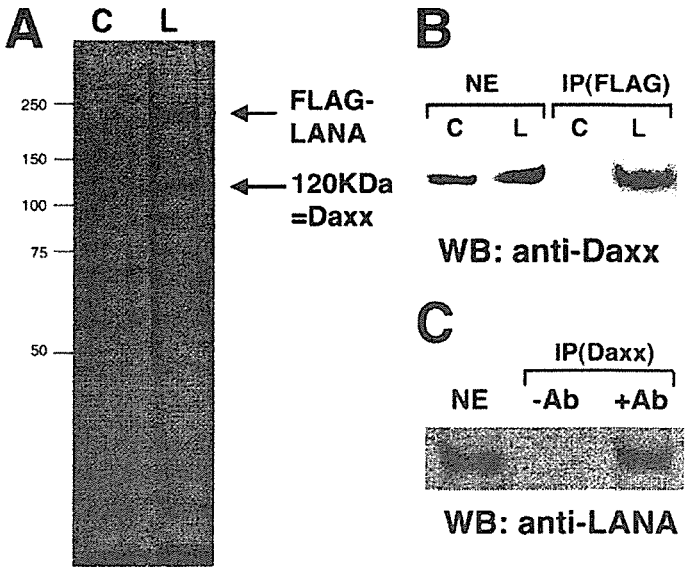

FIGURE 1. **Identification of Daxx as a LANA-binding protein.** *A*, immune complex with anti-FLAG antibody of nuclear extract (*NE*) of HeLa cells was analyzed by SDS-PAGE. Proteins were detected with silver staining. A protein of 120 kDa associated with FLAG-LANA was identified as Daxx. (*C*: control parent HeLa cells, *L*: LANA-expressing HeLa cells). *B*, immune complex with anti-FLAG antibody followed by Western blotting (*WB*) with anti-Daxx antibody. Daxx was detected at about 120 kDa. *C*, immune complex with anti-Daxx antibody followed by Western blotting with anti-LANA antibody using nuclear extract of BCBL-1 cells. A band of about 250 kDa was detected as LANA.

RESULTS

Identification of Daxx as a LANA-binding Protein—To identify host proteins that associate with LANA, we constructed a plasmid expressing FLAG-LANA (N terminus-tagged) to transfect into HeLa cells and established several stable LANA-

expressing clones. We cultured one clone of the LANA-expressing cells and prepared nuclear extract. This extract was incubated with anti-FLAG affinity gel (M2-agarose), followed by elution with FLAG peptides. Eluate was subjected to SDS-PAGE to detect a prominent 120-kDa band (Fig. 1*A*). Although there was a 75-kDa band, which was a nonspecific binding protein commonly found with the antibody. We determined the sequences of the N-terminal 10 residues of the 120-kDa protein, which revealed the protein to be Daxx. To confirm the identification, the nuclear extract (each 500 μg of protein) was immunoprecipitated with anti-FLAG antibody to apply to immunoblotting with anti-Daxx antibody. As shown in Fig. 1*B*, anti-Daxx antibody recognized a band of 120 kDa. These results indicated that Daxx is a cellular binding protein of exogenously expressed LANA in the HeLa cell. To confirm LANA-Daxx interaction in a physiological context, we immunoprecipitated with anti-Daxx antibody from nuclear extracts of BCBL-1 cells, a PEL cell line infected with KSHV. LANA was co-immunoprecipitated with Daxx as well (Fig. 1*C*). This result suggested that LANA formed a complex with Daxx in KSHV-infected cells.

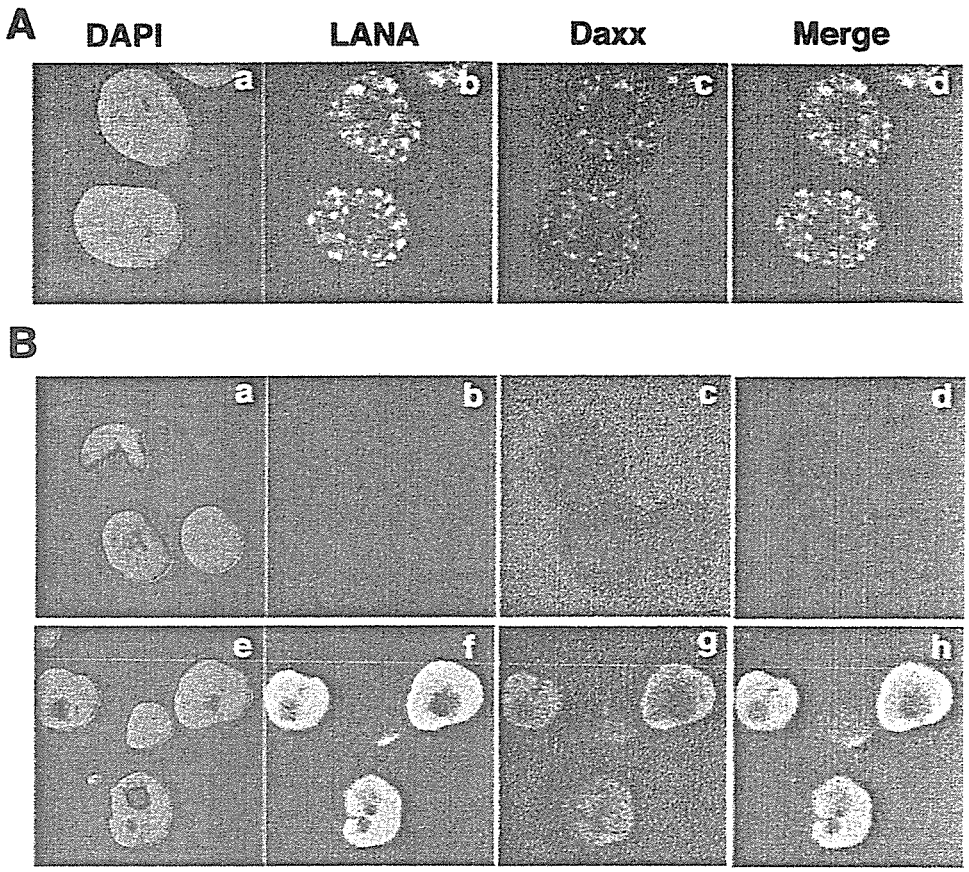

FIGURE 2. **LANA co-localizes with Daxx in BCBL-1 cells and HeLa cells.** Confocal microscopic images of PEL cell line, BCBL-1 cells (*A*), and HeLa cells (*B*, control (*panels a–d*) and LANA-expressing cells (*panels e–h*)). Cells were doubly immunostained with anti-LANA antibody (1:500 for *A*, 1:1000 for *B*) and anti-Daxx antibody (1:100 for *A*, 1:200 for *B*). Images represent cells stained with DAPI (*panels a* and *e*), anti-LANA antibody (*panels b* and *f*), or anti-Daxx antibody (*panels c* and *g*), and merged images of LANA and Daxx staining (*panels d* and *h*).

Colocalization of LANA and Daxx in the Nuclei of KSHV-infected Cell Line BCBL-1—Next we examined the localization of LANA and Daxx in BCBL-1 by immunofluorescence microscopic assay (Fig. 2*A*). LANA gave a characteristic speckled staining pattern in nuclei of the cells (Fig. 2*A*, *panel b*), Daxx also showed some speckles in the nuclei (Fig. 2*A*, *panel c*). The merged image indicated that LANA considerably co-localized with Daxx in the nuclear dots (Fig. 2*A*, *panel d*). We also investigated the localization of Daxx using HeLa cells (Fig. 2*B*). LANA gave fine patchy staining in the nucleus (Fig. 2*B*, *panel f*), which is a typical observation in the absence of KSHV genome (Fig. 2*B*, *panel g*). The parental HeLa cells showed diffused staining of Daxx throughout the cell (Fig. 2*B*, *panel c*). In contrast, Daxx appeared to accumulate in the nuclei of the LANA-expressing cells (used in Fig. 1) (Fig. 2*B*, *panel g*). LANA and Daxx largely localized in the nucleus of the HeLa cells (Fig. 2*B*, *panel h*). We performed biochemical fractionation using three independent clones of LANA-expressing HeLa cells and examined cellular localization of Daxx by Western blotting. The results indicated that the amount of Daxx in the nuclear fraction increased as LANA expression increased, although total amounts of Daxx were comparable in these HeLa clone cells (data not shown).

A Region Containing the Acidic-rich Domain in LANA Is Required for Binding with Daxx—To determine the interacting domain of LANA with Daxx, we constructed a series of LANA deletion mutants (Fig. 3*A*), which were translated *in vitro* and subjected to pull-down assay with GST-Daxx. As shown in Fig. 3*B*, full-length LANA was pulled down with GST-fused full-length Daxx, indicating direct interaction between LANA and Daxx. Three N-terminal mutants of LANA (L1–L3) bound with GST-Daxx, but the shortest N-terminal LANA (aa 1–261) (L4), and C-terminal LANA (aa 496–740) (L5) failed (Fig. 3*B*). We constructed mammalian expression plasmids, LANA-N (aa 1–564), LANA-C (aa 496–1162), LANA-N1 (aa 1–260), LANA-N2 (aa 1–320), LANA-N3 (aa 1–344), and LANA-ΔAD (with aa 322–493 deleted) (Fig. 3*A*). These plasmids were co-transfected with pcDNA-Daxx into 293T cells, and the nuclear extracts were analyzed. Immunoprecipitation with anti-Daxx antibody and Western blotting with anti-FLAG antibody indicated that Daxx formed a complex with full-length LANA and LANA-N, and weakly with LANA-N3, but not with the other LANA fragments (Fig. 3*C*). Taken together, these results suggested that aa 320–344 of LANA, which contains many aspartic acids and glutamic acids, were required for binding with Daxx.

A Central Domain of Daxx Is Required to Interact with LANA—To determine the critical region of Daxx for binding with LANA, a series of GST-fused deletion mutants of Daxx (Fig. 4*A*)

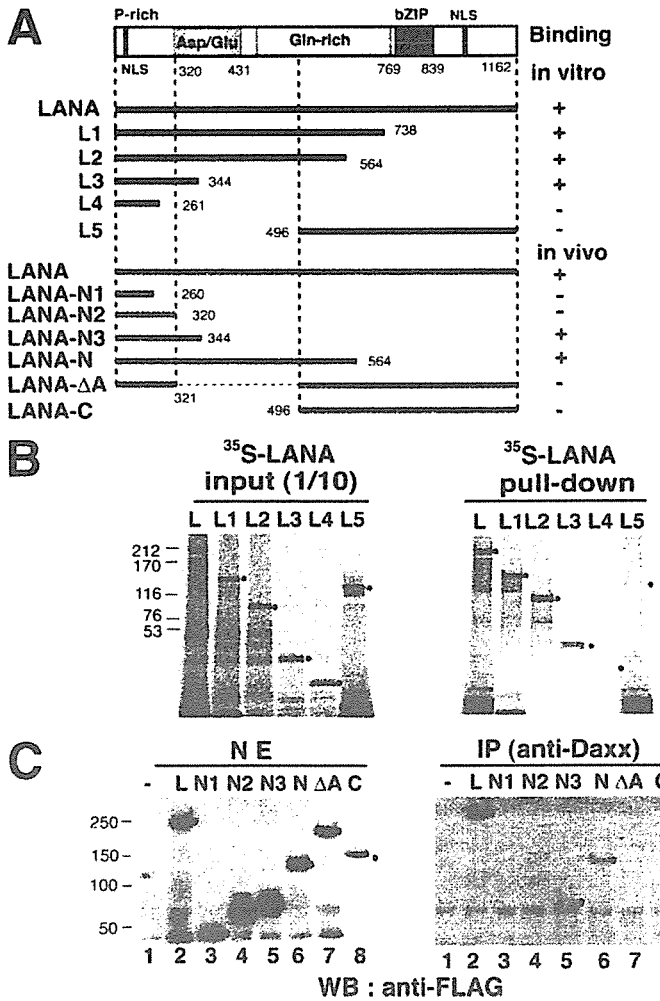

FIGURE 3. **A region containing an acidic-rich domain in LANA is required for binding with Daxx *in vitro* and *in vivo*.** *A*, domain structure of LANA and its deletion mutants. LANA is constituted of domains of proline-rich, acidic-rich, glutamine-rich, and basic leucine-zipper. A series of deletion mutants of LANA and the binding activity *in vitro* and *in vivo* are shown. *B*, result of pull-down assay with GST-fused full-length Daxx of ^{35}S-labeled LANA deletion mutants (*L1–L5*). *C*, co-immunoprecipitation of Daxx and LANA deletion mutants in 293T cells. PFLAG-CMV-2 vector (4.0 μg) (*lane 1*), pFLAG-LANA (4.0 μg) (*lane 2*), pFLAG-LANA-N1 (1.0 μg) (*lane 3*), pFLAG-LANA-N2 (2.0 μg) (*lane 4*), pFLAG-LANA-N3 (2.0 μg) (*lane 5*), pFLAG-LANA-N (2.0 μg) (*lane 6*), pFLAG-LANA-ΔA (4.0 μg) (*lane 7*), or pFLAG-LANA-C (4.0 μg) (*lane 8*) was individually co-transfected with pcDNA-Daxx (1.0 μg) in 60-mm dishes with adjustment of total DNA amount (5.0 μg). The immunoprecipitates (*IP*) with anti-Daxx antibody were followed by immunoblotting (*WB*) with anti-FLAG antibody (M5).

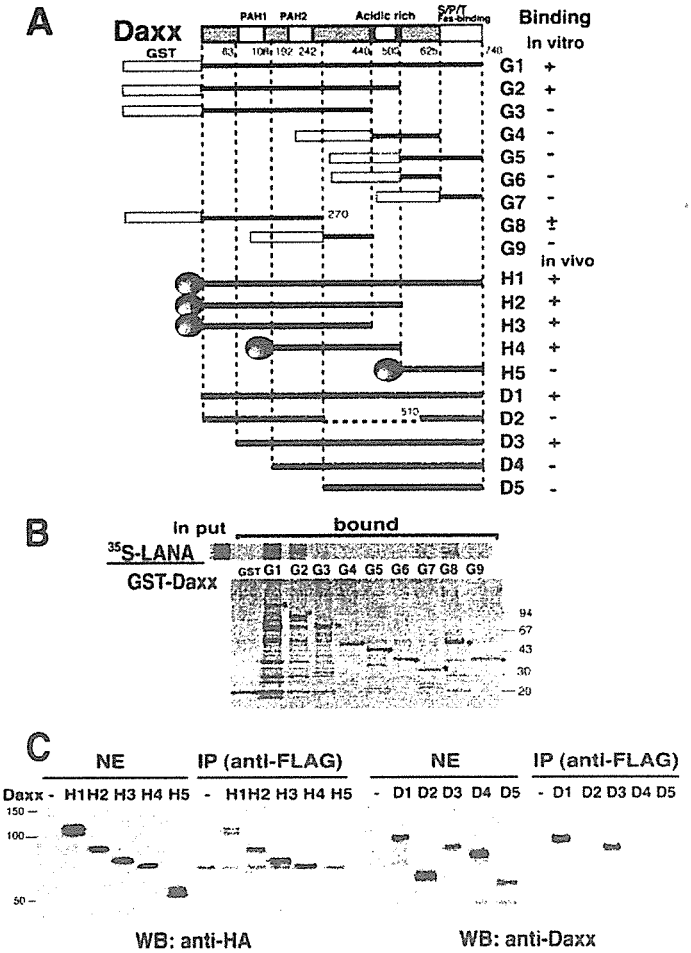

FIGURE 4. *A*, central region containing PAH 2 and acidic-rich domain in Daxx is required to interact with LANA. *A*, domain structure of Daxx and various deletion mutants. Daxx is composed of two PAH and acidic-rich and Ser/Pro/Thr-rich domains. A series of mutants of Daxx and the binding activity *in vitro* and *in vivo* are shown. *B*, purified GST-Daxx variants (*G1–G9*) were applied in *in vitro* pull-down assay with full-length ^{35}S-LANA. *C*, mammalian expression plasmids, pCMV-HA-Daxx-H1 (full-length) (2.0 μg), pCMV-HA-Daxx-H2 (aa 1–500) (2.0 μg), pCMV-HA-Daxx-H3 (aa 1–440) (1.0 μg), pCMV-HA-Daxx-H4 (aa 110–500)(1.0 μg), pCMV-HA-Daxx-H5 (aa 500–740) (1.0 μg) were co-transfected with pFLAG-LANA (1.0 μg) (*left two panels*). PcDNA-Daxx-D1 (full-length) (1.0 μg), pcDNA-Daxx-D2 (deleted aa 271–509) (3.0 μg), pcDNA-Daxx-D3 (aa 63–740)(3.0 μg), pcDNA-Daxx-D4 (aa 111–740)(3.0 μg), and pcDNA-Daxx-D5 (aa 243–740) (2.0 μg) were individually co-transfected with pFLAG-LANA (1.0 μg) (*right two panels*). Immunoprecipitates (*IP*) with anti-FLAG antibody (M2) were followed by Western blotting (*WB*) with anti-HA antibody (*left panels*) or anti-Daxx antibody (*right panels*).

were produced in *E. coli*, and applied to pull-down assay with full-length ^{35}S-labeled LANA. The GST-fused full-length Daxx (G1) and the Daxx-deleted aa 500–740 (G2) bound to LANA, but deleted aa 440–740 (G3) failed (Fig. 4*B*). From the *in vitro* result above, the region of aa 440–500 in Daxx was thought to be critical for the binding. However, GST-fused aa 440–625 of Daxx (G4) did not bind (Fig. 4*B*), nor did any other mutants, although weak binding was observed with GST-fused aa 1–270 of Daxx (G8)(Fig. 4*B*). We constructed a series of deletion mutants of N-terminal HA-tagged Daxx (H2–H5), and co-expressed them with pFLAG-LANA in 293T cells. Immunoprecipitation with anti-FLAG antibody followed by Western blotting with anti-HA antibody showed that all the mutants except H5 bound to LANA (Fig. 4*C*, *left two panels*). The acidic-rich region (aa 440–500) of Daxx was not critical to the binding with LANA in cells, not corresponding with the results *in vitro*. To examine contribution of N terminus of Daxx, a series of mutant Daxx expression vectors with N-terminal deletion (D3–D5) and a deletion mutant without central region aa 271–509 (D2), were constructed and transiently expressed in 293T cells. Experiments of immunoprecipitation with anti-FLAG antibody and Western blotting with anti-Daxx antibody (sc-7152, that recognizes the C terminus of Daxx) showed that D3 bound firmly with LANA, but D4 did very little (Fig. 4*C*, *right two panels*). The first paired amphipathic helix (PAH), aa 63–108 appeared to be of some importance for the binding, although HA-tagged Daxx without PAH1 (H4) bound LANA. These results indicated that a central region aa 63–440 within Daxx,

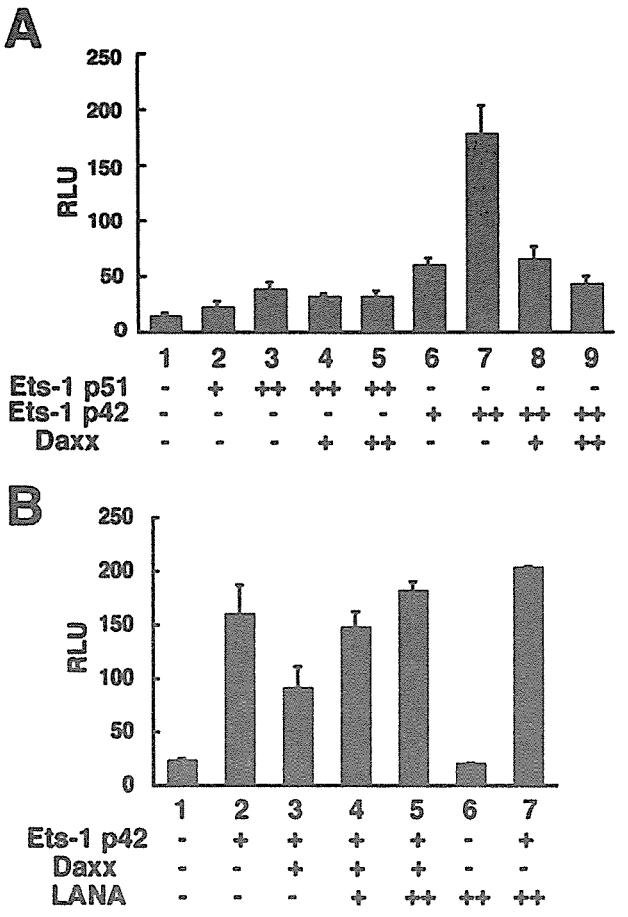

FIGURE 5. **LANA inhibited Daxx-mediated repression on Ets-1-dependent VEGF receptor 1 (Flt-1) gene expression.** *A*, Daxx repressed Ets-1-dependent Flt-1 expression. PcDNA-p51Ets-1 or pcDNA-p42Ets-1 (+; 25 ng, ++; 50 ng) were co-transfected with pcDNA-Daxx (+; 200 ng, ++; 500 ng) and pFlt-luc (100 ng). *B*, LANA counteracts Daxx-mediated repression in Flt-1 expression in the presence or absence of exogenous Daxx. PcDNA-p42Ets-1 (50 ng), pcDNA-Daxx (200 ng), and pFLAG-LANA (0, +; 50, ++; 100 ng, respectively) were co-transfected with pFlt-1-luc (100 ng). The relative luciferase activity (*RLU*) was normalized by β-galactosidase activity. Assays were performed in triplicate, and *error bars* indicate S.D.

containing two paired PAHs and its following 200 aa, was important for the binding with LANA in cells.

LANA Inhibited Daxx-mediated Repression of Ets-1-dependent VEGF Receptor 1 (Flt-1) Gene Expression— To examine the role of Daxx in Kaposi's sarcoma, we focused on Ets-1 transcription factor. It was reported that Daxx interacts with Ets-1 to repress Ets-1-dependent transcriptional activity of MMP-1 and Bcl-2 (12). On the other hand, as a characteristic feature of KS, it is known that VEGF and its receptors, Flt-1 and KDR (VEGF receptor-1 and -2, respectively), are highly expressed in KS (20). There are several Ets-1 motifs in Flt-1 and KDR promoters to regulate the expression (26) (27). We examined the effect of Daxx on Ets-1-dependent Flt-1 expression. We co-transfected a luciferase reporter plasmid pFlt-1-luc driven by Flt-1 promoter, an Ets-1 expression vector, and a Daxx expression vector into 293T cells, to perform luciferase assay. Transcriptional activity on Flt-1 increased depending on the amount of Ets-1 plasmid, although the effect of p51-Ets-1 was quite weak. Daxx evidently repressed Ets-1-dependent activation (Fig. 5*A*). p51 and p42 are two human variants of the Ets-1 molecule. It is reasonable that the activity of p51-Ets-1 is lower than p42-Ets-1 because p42-Ets-1 lacks exon VII, the internal transcriptional regulatory domain (24). This result is similar to the case of MMP-1 and Bcl-2 expression (28). As we observed the repressive activity of Daxx on Ets-1-dependent Flt-1 expression, we examined the effect of LANA on the Daxx-mediated repression with p42Ets-1. Co-transfection with a LANA expression plasmid dose-dependently reactivated the transcriptional activity repressed by exogenous Daxx (Fig. 5*B*, *4* and *5*), although LANA slightly activated it in the absence of exogenous Daxx (Fig. 5*B*, *7*). These results suggested that LANA inhibited the repression via interaction with Daxx.

LANA Activated Expression of VEGF Receptors in Vascular Endothelial Cells—To investigate the possibility that LANA induces Flt-1 in Kaposi's sarcoma lesion, we tried to express LANA in HUVEC, because endothelial cells (ECs) are regarded as the origins of KS lesions. We constructed a plasmid, pIRES2-LANA-GFP, which contains an internal ribosomal entry site (IRES) to express both LANA and GFP from a single mRNA. We transfected pIRES2-LANA-GFP or pIRES2-GFP as control into HUVEC and Flt-1 and KDR expression in GFP-positive cells were analyzed by flow cytometry. Flt-1 of GFP-positive cells in pIRES2-LANA-GFP-transfected cells was significantly increased as compared with that in control cells (Fig. 6*A*, *left*). The number of cells expressing Flt-1 over log intensity 1 (M1) was about 1.9× higher (Fig. 6*A*, *upper, right graph*) than that of control. M1 of KDR also increased 1.4× (Fig. 6*A*, *lower, right graph*). Furthermore, to examine the level of mRNA of the two receptors, we performed real-time PCR with total RNA prepared from the GFP-expressing HUVEC. LANA expression in pIRES2-LANA-GFP-transfected cells was confirmed by using PCR with primers of LANA (data not shown). The relative expressions of Flt-1 and KDR in LANA-expressing cells were 1.4 and 2.0× higher than that of control cells, respectively (Fig. 6*B*). Although there was discrepancy between rise of protein and mRNA, results of both FACS and real-time PCR indicated that LANA induced the two receptors in human endothelial cells. The expression of Ets-1 and Daxx was not altered between LANA-expressing cells and control cells (Fig. 6*B*).

LANA Sequesters Daxx from Ets-1—To resolve the mechanism of the activation of VEGF receptors expression by LANA, we examined the relation of the three molecules, LANA, Daxx, and Ets-1. 293T cells were co-transfected with a constant amount of pcDNA-Daxx and pcDNA-Ets-1, and a variable amount of pFLAG-LANA. Nuclear extracts were prepared and subjected to immunoprecipitation and Western blotting with anti-Ets-1 antibody, anti-Daxx antibody or anti-FLAG antibody. Daxx and Ets-1 were expressed in a fixed amount (Fig. 7*A*, *row a*), *middle and right panel*, respectively) and FLAG-LANA was dose-dependently increased in the nuclear extract (Fig. 7*A*, *row a, left panel*). When we performed immunoprecipitation with anti-FLAG antibody, Daxx was detected in the immune complex in proportion to the amount of LANA (Fig. 7*A*, *row b, middle panel*). On the other hand, we detected no specific interaction between LANA and Ets-1 in the immune complex (Fig. 7*A*, *row b, right panel*). Next, by immunoprecipitation with anti-Daxx antibody, FLAG-LANA was detected in direct proportion to the amount of LANA (Fig. 7*A*, *row c, left panel*). The immune complex also contained Ets-1 in inverse

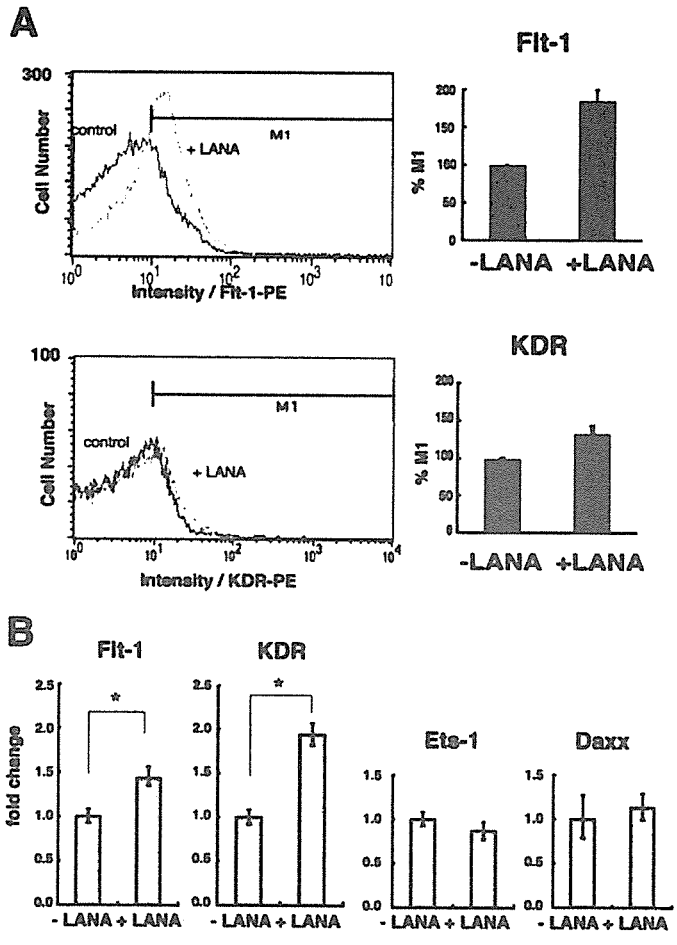

FIGURE 6. **LANA induced VEGF receptors in HUVEC.** *A*, flow cytometric analysis of Flt-1 (*upper graphs*) and KDR (*lower graphs*) expression of control (pIRES2-GFP transfected cells; *black lines*) and LANA-expressing cells (pIRES2-LANA-GFP-transfected cells; *gray lines*). The graphs to the *right* of each indicate percentages of cells that exceed 1 of the relative log intensity (*M1*). Experiments were repeated three times and the M1 values represent means of the three experiments; *error bars* indicate S.D. *B*, real-time PCR analysis of Flt-1, KDR, Ets-1, and Daxx. HUVECs transfected transiently with pIRES2-LANA-GFP or pIRES2-GFP (as a control) were sorted 2 days after transfection. Total RNA extracted from the cells (1 μg) was reverse-transcribed to cDNA (40 μl), and aliquots (0.4 μl) were applied to real-time PCR (20 μl) with each primer (0.4 mM) in triplicate described under "Experimental Procedures." Values represented relative expression of Flt-1, KDR, Ets-1, and Daxx (calculated with threshold cycle number, CT) of LANA-expressing cells compared with that of control cells. Each value was adjusted with CT of internal control (GAPDH). *, p value < 0.02.

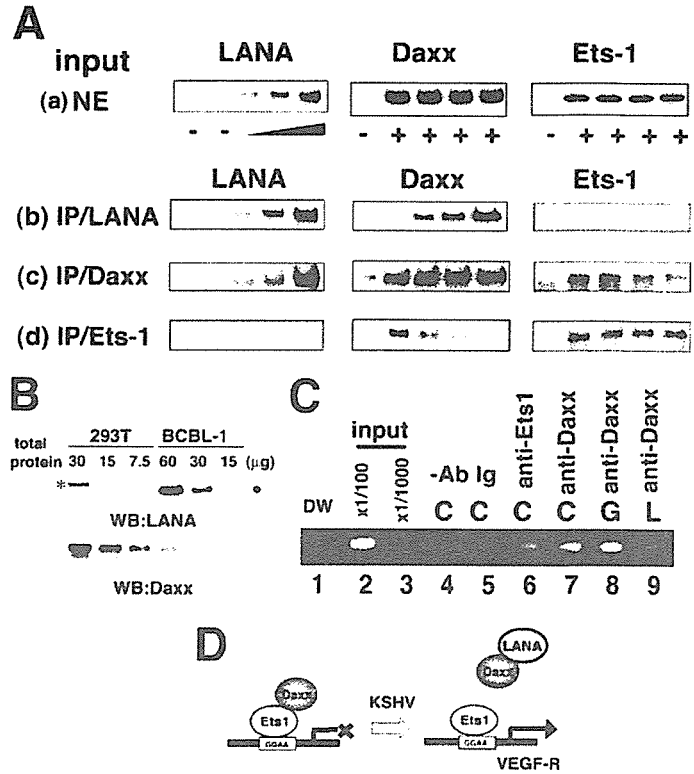

FIGURE 7. **LANA interacted with Daxx to sequester from Ets-1.** *A*, Western blotting analysis of immunoprecipitates with anti-FLAG, anti-Daxx, and anti-Ets-1 antibodies. 293T cells were transfected with a constant amount of pcDNA-Daxx (2 μg) and pcDNA-p42Ets-1 (2 μg), and an increasing amount of pFLAG-LANA (0.25, 0.5, 1.0 μg). Total DNA amounts were adjusted with pFLAG-CMV-2 vector to be 5 μg. Nuclear extracts (*row a*), immune complex using anti-FLAG antibody (*row b*), immune complex using anti-Daxx antibody (*row c*), and immune complex using anti-Ets-1 antibody (*row d*), were subject to Western blotting with anti-FLAG antibody (*left*), anti-Daxx antibody (*middle*) or anti-Ets-1 antibody (*right*). *B*, relative protein amounts of LANA and Daxx in BCBL-1 cells and those of transfected 293T cells. 293T cells were co-transfected with pcDNA-Daxx (2 μg), pcDNA-p42Ets-1 (2 μg), and pFLAG-LANA (1.0 μg). Nuclear extract (30, 15, 7.5 μg of the 293T cells and 60, 30, 15 μg of BCBL-1 cells) were subjected to Western blotting with anti-LANA antibody or anti-Daxx antibody. FLAG-LANA (*) migrated slower than native LANA(●) did. *C*, chromatin immunoprecipitation of Ets-1 and Daxx interaction with Flt-1 promoter in HUVECs. Bands indicate PCR products targeting −90 to +8 of Flt-1 promoter. 2 μl of water (*lane 1*), 1/100 and 1/1000 of input (cross-linked and sonicated pre-immunoprecipitation lysate) (*lanes 2* and *3*), eluate from no antibody (*lane 4*), rabbit IgG (2 μg) (*lane 5*), anti-Ets-1 antibody (2 μg) (*lane 6*), and anti-Daxx antibody (2 μg) (*lane 7*) were applied to the PCR reaction, respectively. Eluate from anti-Daxx antibody of LANA-expressing HUVECs (*L*, *lane 9*) and that from the control GFP-expressing HUVECs (*G*, *lane 8*) were subjected to PCR reaction. *D*, possible mechanism for induction of VEGF receptors by LANA. Daxx interacts with Ets-1, and represses Ets-1-dependent expression in the absence of LANA, while LANA sequesters Daxx from Ets-1 to inhibit the interaction between Daxx and Ets-1, resulting in activation of Ets-1-dependent expression of VEGF receptors.

proportion to LANA expression (Fig. 7*A*, *row c*, *right panel*). Consistently, Daxx was detected in the immune complex with anti-Ets-1 antibody in inverse proportion to LANA expression (Fig. 7*A*, *row d*, *middle panel*). LANA was not detected in the immune complex with the anti-Ets-1 antibody (Fig. 7*A*, *row d*, *left panel*), which implies that increasing LANA caused increase of Daxx-LANA interaction, and reduction of Daxx-Ets-1 interaction. These results suggested that LANA sequesters Daxx from Ets-1, which results in inhibition of the interaction between Daxx and Ets-1.

In the experiments above we used transiently transfected 293T cells (Fig. 7*A*). To address whether the transient expression system for LANA-Daxx interaction is physiologically relevant or not, we analyzed relative expression levels of LANA and Daxx proteins using BCBL-1 and the transfected 293T cells. As shown in Fig. 7*B*, the expression level of exogenous LANA protein in 293T cells in the same condition of Fig. 7*A* was similar to that of endogenous LANA in BCBL-1 cells. In contrast, endogenous Daxx expression level is much lower in BCBL-1 cells than in the 293T cells. These data indicated that relative expression ratio of endogenous LANA to Daxx in BCBL-1 cells was much higher than that of LANA-transfected 293T cells.

Daxx associated with Flt-1 promoter and LANA reduced its association in HUVEC. To investigate the possibility that Daxx affects transcriptional activity of Ets-1 for Flt-1 expression in endothelial cells (ECs), we performed ChIP assay using HUVEC. Cross-linked nuclear extract from HUVECs was immunoprecipitated with anti-Ets-1 antibody or anti-Daxx

antibody, and subjected to PCR to amplify a 98-bp fragment. The PCR product is designed to span the fourth ets motif (−54 to −51) that is thought to be indispensable for Flt-1 promoter activity (26). The anti-Daxx antibody precipitated the Flt-1 promoter as well as anti-Ets-1 antibody (Fig. 7*C*, *lanes 6* and *7*). The result indicated that Daxx as well as Ets-1 associated with Flt-1 promoter in ECs. Furthermore, HUVECs transfected with pIRES2-LANA-GFP or pIRES2-GFP as the control were sorted and subjected to ChIP assay with anti-Daxx antibody. The PCR product from the LANA-expressing cells (Fig. 7*C*, *L*, *lane 9*) was lower than that of control GFP-expressing cells (Fig. 7*C*, *G*, *lane 8*), indicating reduction of Daxx association with the promoter of the *Flt-1* gene in ECs.

DISCUSSION

LANA is reported to have multiple functions in KS lesion. It interacts with many host cellular molecules: p53 (8), pRb (9), ATF4/CREB2 (29), CBP (30), c-Jun (31), RING3 (32), mSin3A (33), HP-1 (33), Dek (34), GSK-3b (10) and so on. In the present study, we identified Daxx as a new member of LANA-binding proteins. Daxx was prominently detected in our immunoaffinity system, but this system also detected previously reported LANA-interacting protein such as RING3 by Western blotting (data not shown). We showed the interaction between the two proteins *in vivo* (Fig. 1) and *in vitro* (Figs. 3 and 4), which indicates that Daxx and LANA directly bound to each other. Fluorescent immunostaining assay showed co-localization of LANA and Daxx in BCBL-1 cells, supporting LANA-Daxx interaction in cells (Fig. 2).

Daxx is reported to bind many cellular molecules, indicating its involvement in multiple cellular processes. Although Daxx could interact with proteins of cytoplasm or membrane, it also interacted with some transcription factors and localized sometimes in the nuclear matrix structure, PML NBs (promyelocytic leukemia nuclear bodies). PML NBs are thought to provide platforms for transcription regulation, DNA repair, apoptosis, DNA replication, RNA transport, and many viruses target PML NBs to pirate host functions (reviewed by Everett, Ref. 35). Ets-1 associates with a PML NBs protein, Sp100 (36). Therefore, it might be a strategy of KSHV that LANA targets Daxx of PML NBs to modulate the cellular function(s) of Ets-1.

Although most LANA-binding proteins are reported to interact through the C or N terminus of LANA, the critical domain for binding with Daxx seemed to be a central region, aa 321–344 of LANA (Fig. 3). The aa 320–431 of LANA consists mainly of aspartic acid and glutamic acid. It is reported that a transcriptional co-activator, CBP interacts through this acidic-rich region of LANA (30). This domain may have some roles in transcriptional regulation. On the other hand, although most Daxx-binding proteins interact around the C terminus of Daxx, a central domain containing the PAHs and the following region of Daxx appeared to be important for binding with LANA *in vivo* (Fig. 4). There was a discrepancy between *in vitro* and *in vivo* binding. Protein modification may be one possibility explaining *in vivo* binding activity. It is reported that Daxx is modified by hyperphosphorylation (13) and sumoylation (37). Because the sumoylation sites of Daxx are reported to be Lys^{630} and Lys^{631}, it is unlikely to affect the interaction. The hyperphosphorylation site on Daxx has not been identified, but it is possible to be related to the binding. There may be other possibilities, for example, constructive interference by fused GST protein. PAH is a characteristic domain that is involved in transcriptional co-repressors such as mSin3 (38). It is interesting that mSin3A binds to aa 1–340 of LANA (28). There is a report that acetylated histone H4 interacts through PAH1 within Daxx, but no report that any other host molecule binds through this region of Daxx. As Daxx interacts with Ets-1 through the C-terminal region of Daxx (12), there may be no direct competition for Daxx between LANA and Ets-1.

Based on the interaction between LANA and Daxx (Figs. 1–4), we found that LANA induced VEGF receptors in ECs (Fig. 6) in accordance with the results of reporter assays (Fig. 5). Although expression level changes were not consistent for Flt-1 and KDR in protein (Fig. 6*A*) and mRNA (Fig. 6*B*), it may be caused by time point difference. This is the first report of the function of LANA in angiogenesis. It is reported that KSHV ORF74 (viral G-protein coupled receptor, v-GPCR) contributes to expression of VEGF receptors (39). Because ORF74 is expressed in the viral lytic infection cycle, it is unlikely that ORF74 is the only gene of KHSV that induces angiogenesis in KS. It is likely that some other factors such as VEGF and hypoxia-inducible factor (HIF) additionally affect on expression of these receptors in KS (40) (41).

As to the mechanism of activation of the receptor expression by LANA, we propose a hypothesis that LANA sequesters Daxx from Ets-1 (Fig. 7*D*), based on the results of co-immunoprecipitation (Fig. 7*A*) and ChIP assay (Fig. 7*C*). LANA slightly activated Ets-1 dependent Flt-1 expression without exogenous Daxx in the reporter assay (Fig. 5*B*). It is thought that LANA sequestered endogenous Daxx. However it is possible that LANA activates Flt-1 expression through an unidentified mechanism(s). At least LANA did not activate Flt-1 expression through up-regulation of Ets-1 expression (Fig. 6*B*). In human Flt-1 promoter, there are five Ets motifs and a CRE (cAMP response element). It is reported that co-existence of the fourth Ets motif, and the CRE is necessary for Flt-1 expression (26). LANA is reported to modulate the expression of a reporter plasmid with CRE, but the effect of LANA on CRE is repression (29). There is no CRE in the promoter of KDR.

Given that LANA induces VEGF receptors in KS lesion, we propose this hypothesis: Daxx binds Ets-1 to repress expression of VEGF receptors in normal ECs, while in KSHV-infected cells, LANA binds to Daxx to inhibit Daxx-Ets-1 interaction, resulting in the activation of Ets-1-dependent VEGF receptors. Furthermore, LANA-Daxx interaction might contribute to not only VEGF receptor gene expression but also to other Daxx-mediated gene regulation related to the pathogenesis of KS, PEL, and MCD malignancy.

Acknowledgments—We thank Dr. Kaoru Morishita (Daiichi Pharmaceutical Co., Ltd., Tokyo), and Dr. Runzhao Li (Medical University of South Carolina) for kindly providing plasmids. We thank Dr. Harutaka Katano (Department of Pathology, National Institute of Infectious Diseases) for providing BCBL-1 cells and useful advice, Dr. Kazuo Suzuki (Department of Bioactive Molecules, National Institute of Infectious Diseases) for useful discussion, and Eri Watanabe, Junko Kondo, and Yuki Hashimoto for their technical assistance.

REFERENCES

1. Flore, O., Rafii, S., Ely, S., O'Leary, J. J., Hyjek, E. M., and Cesarman, E. (1998) *Nature* **394,** 588–592
2. Moore, P. S., and Chang, Y. (1998) *Am. J. Epidemiol.* **147,** 217–221
3. Dupin, N., Fisher, C., Kellam, P., Ariad, S., Tulliez, M., Franck, N., van Marck, E., Salmon, D., Gorin, I., Escande, J. P., Weiss, R. A., Alitalo, K., and Boshoff, C. (1999) *Proc. Natl. Acad. Sci. U. S. A.* **96,** 4546–4551
4. Russo, J. J., Bohenzky, R. A., Chien, M. C., Chen, J., Yan, M., Maddalena, D., Parry, J. P., Peruzzi, D., Edelman, I. S., Chang, Y., and Moore, P. S. (1996) *Proc. Natl. Acad. Sci. U. S. A.* **93,** 14862–14867
5. Katano, H., Sato, Y., Kurata, T., Mori, S., and Sata, T. (1999) *Am. J. Pathol.* **155,** 47–52
6. Ballestas, M. E., Chatis, P. A., and Kaye, K. M. (1999) *Science* **284,** 641–644
7. Garber, A. C., Shu, M. A., Hu, J., and Renne, R. (2001) *J. Virol.* **75,** 7882–7892
8. Friborg, J., Jr., Kong, W., Hottiger, M. O., and Nabel, G. J. (1999) *Nature* **402,** 889–894
9. Radkov, S. A., Kellam, P., and Boshoff, C. (2000) *Nat. Med.* **6,** 1121–1127
10. Fujimuro, M., Wu, F. Y., ApRhys, C., Kajumbula, H., Young, D. B., Hayward, G. S., and Hayward, S. D. (2003) *Nat. Med.* **9,** 300–306
11. Yang, X., Khosravi-Far, R., Chang, H. Y., and Baltimore, D. (1997) *Cell* **89,** 1067–1076
12. Li, R., Pei, H., Watson, D. K., and Papas, T. S. (2000) *Oncogene* **19,** 745–753
13. Hollenbach, A. D., Sublett, J. E., McPherson, C. J., and Grosveld, G. (1999) *EMBO J.* **18,** 3702–3711
14. Emelyanov, A. V., Kovac, C. R., Sepulveda, M. A., and Birshtein, B. K. (2002) *J. Biol. Chem.* **277,** 11156–11164
15. Kim, E. J., Park, J. S., and Um, S. J. (2003) *Nucleic Acids Res.* **31,** 5356–5367
16. Oikawa, T., and Yamada, T. (2003) *Gene (Amst.)* **303,** 11–34
17. Sacchi, N., de Klein, A., Showalter, S. D., Bigi, G., and Papas, T. S. (1988) *Leukemia* **2,** 12–18
18. Wernert, N., Raes, M. B., Lassalle, P., Dehouck, M. P., Gosselin, B., Vandenbunder, B., and Stehelin, D. (1992) *Am. J. Pathol.* **140,** 119–127
19. Masood, R., Cai, J., Zheng, T., Smith, D. L., Naidu, Y., and Gill, P. S. (1997) *Proc. Natl. Acad. Sci. U. S. A.* **94,** 979–984
20. Masood, R., Cesarman, E., Smith, D. L., Gill, P. S., and Flore, O. (2002) *Am. J. Pathol.* **160,** 23–29
21. Sato, Y., Kanno, S., Oda, N., Abe, M., Ito, M., Shitara, K., and Shibuya, M. (2000) *Ann. New York Acad. Sci.* **902,** 201–205; discussion 205–207
22. Tang, D. G., and Conti, C. J. (2004) *Semin. Thromb. Hemost.* **30,** 109–117
23. Morishita, K., Johnson, D. E., and Williams, L. T. (1995) *J. Biol. Chem.* **270,** 27948–27953
24. Koizumi, S., Fisher, R. J., Fujiwara, S., Jorcyk, C., Bhat, N. K., Seth, A., and Papas, T. S. (1990) *Oncogene* **5,** 675–681
25. Yamagoe, S., Kanno, T., Kanno, Y., Sasaki, S., Siegel, R. M., Lenardo, M. J., Humphrey, G., Wang, Y., Nakatani, Y., Howard, B. H., Ozato, K., Xu, R. H., Peng, Y., Fan, J., Yan, D., Princler, G., Sredni, D., and Kung, H. F. (2003) *Mol. Cell. Biol.* **23,** 1025–1033
26. Wakiya, K., Begue, A., Stehelin, D., and Shibuya, M. (1996) *J. Biol. Chem.* **271,** 30823–30828
27. Kappel, A., Schlaeger, T. M., Flamme, I., Orkin, S. H., Risau, W., and Breier, G. (2000) *Blood* **96,** 3078–3085
28. Krithivas, A., Young, D. B., Liao, G., Greene, D., and Hayward, S. D. (2000) *J. Gen. Virol.* **74,** 9637–9645
29. Lim, C., Sohn, H., Gwack, Y., and Choe, J. (2000) *J. Gen. Virol.* **81,** 2645–2652
30. Lim, C., Gwack, Y., Hwang, S., Kim, S., and Choe, J. (2001) *J. Biol. Chem.* **276,** 31016–31022
31. An, J., Sun, Y., and Rettig, M. B. (2004) *Blood* **103,** 222–228
32. Platt, G. M., Simpson, G. R., Mittnacht, S., and Schulz, T. F. (1999) *J. Virol.* **73,** 9789–9795
33. Lim, C., Lee, D., Seo, T., Choi, C., and Choe, J. (2003) *J. Biol. Chem.* **278,** 7397–7405
34. Krithivas, A., Fujimuro, M., Weidner, M., Young, D. B., and Hayward, S. D. (2002) *J. Virol.* **76,** 11596–11604
35. Everett, R. D. (2001) *Oncogene* **20,** 7266–7273
36. Wasylyk, C., Schlumberger, S. E., Criqui-Filipe, P., and Wasylyk, B. (2002) *Mol. Cell. Biol.* **22,** 2687–2702
37. Jang, M. S., Ryu, S. W., and Kim, E. (2002) *Biochem. Biophys. Res. Commun.* **295,** 495–500
38. Spronk, C. A., Tessari, M., Kaan, A. M., Jansen, J. F., Vermeulen, M., Stunnenberg, H. G., and Vuister, G. W. (2000) *Nat. Struct. Biol.* **7,** 1100–1104
39. Bais, C., VanGeelen, A., Eroles, P., Mutlu, A., Chiozzini, C., Dias, S., Silverstein, R. L., Rafii, S., and Mesri, E. A. (2003) *Cancer Cell* **3,** 131–143
40. Chen, Z., Fisher, R. J., Riggs, C. W., Rhim, J. S., and Lautenberger, J. A. (1997) *Cancer Res.* **57,** 2013–2019
41. Elvert, G., Kappel, A., Heidenreich, R., Englmeier, U., Lanz, S., Acker, T., Rauter, M., Plate, K., Sieweke, M., Breier, G., and Flamme, I. (2003) *J. Biol. Chem.* **278,** 7520–7530

Oncogene (2006) 25, 5113–5124

www.nature.com/onc

ORIGINAL ARTICLE

Nucleolin is involved in interferon regulatory factor-2-dependent transcriptional activation

A Masumi[1], H Fukazawa[2], T Shimazu[3], M Yoshida[3], K Ozato[4], K Komuro[1] and K Yamaguchi[1]

[1]Department of Safety Research on Blood and Biological Products, National Institute of Infectious Diseases, Tokyo, Japan; [2]Department of Bioactive Molecules, National Institute of Infectious Diseases, Tokyo, Japan; [3]Chemical Genetics Laboratory, RIKEN, Saitama, Japan and [4]Laboratory of Molecular Growth and Regulation, National Institute of Child Health and Human Development, National Institute of Health, Bethesda, MD, USA

We have previously shown that interferon regulatory factor-2 (IRF-2) is acetylated in a cell growth-dependent manner, which enables it to contribute to the transcription of cell growth-regulated promoters. To clarify the function of acetylation of IRF-2, we investigated the proteins that associate with acetylated IRF-2. In 293T cells, the transfection of p300/CBP-associated factor (PCAF) enhanced the acetylation of IRF-2. In cells transfected with both IRF-2 and PCAF, IRF-2 associated with endogenous nucleolin, while in contrast, minimal association was observed when IRF-2 was transfected with a PCAF histone acetyl transferase (HAT) deletion mutant. In a pull-down experiment using stable transfectants, acetylation-defective mutant IRF-2 (IRF-2K75R) recruited nucleolin to a much lesser extent than wild-type IRF-2, suggesting that nucleolin preferentially associates with acetylated IRF-2. Nucleolin in the presence of PCAF enhanced IRF-2-dependent *H4* promoter activity in NIH3T3 cells. Nucleolin knock-down using siRNA reduced the IRF-2/PCAF-mediated promoter activity. Chromatin immunoprecipitation analysis indicated that PCAF transfection increased nucleolin binding to IRF-2 bound to the *H4* promoter. We conclude that nucleolin is recruited to acetylated IRF-2, thereby contributing to gene regulation crucial for the control of cell growth.
Oncogene (2006) **25**, 5113–5124. doi:10.1038/sj.onc.1209522; published online 3 April 2006

Keywords: IRF-2; nucleolin; acetylation

Introduction

Interferon regulatory factors (IRFs) have been studied in the context of host defense and oncogenesis (Taniguchi *et al.*, 2001) and transcriptional regulation (Schaffer *et al.*, 1997). Interferon regulatory factor-2 (IRF-2) has generally been described as a transcriptional repressor, and is thought to function by competing with the transcriptional activator IRF-1. However, IRF-2 can act as a positive regulator for interferon stimulated response element (ISRE)-like sequences such as the promoters *H4* (Vaughan *et al.*, 1998; Xie *et al.*, 2001), vascular adhesion molecule-1 and gp91phox (Luo and Skalnik, 1996) as well as Fas ligand (Chow *et al.*, 2000). Biologically, IRF-2 plays an important role in cell growth regulation, and has been shown to be a potential oncogene (Yamamoto *et al.*, 1994). A recent report indicated that IRF-2 drives megakaryocytic differentiation through regulation of the thrombopoietin receptor promoter (Stellacci *et al.*, 2004). It has been reported that many transcription factors, such as MyoD, β-catenin, p53, Tat and CTIIA regulate specific promoters associated with the coactivators p300 and p300/CBP-associated factor (PCAF), and that this regulation leads to specific biological functions (Lakin and Jackson, 1999; Deng *et al.*, 2000; Spilianakis *et al.*, 2000; Polwsskaya *et al.*, 2001; Wolf *et al.*, 2002). Certain IRF proteins interact with other transcription factors such as TFIIB, and the coactivators p300 and PCAF (Wang *et al.*, 1996; Yoneyama *et al.*, 1998; Masumi *et al.*, 1999) and these interactions lead to transcriptional activation or repression depending on the cell types involved. To clarify the regulatory functions of transcription factors, many investigators have studied the coactivators, such as p300 and PCAF.

There are many reports of the histone acetyltransferases such as PCAF, p300/CBP and GCN5 acting as co-activators (Benkirane *et al.*, 1998; Vassilev *et al.*, 1998; Hamamori *et al.*, 1999; Jiang *et al.*, 1999; Masumi *et al.*, 1999; Schiltz *et al.*, 1999; Harrod *et al.*, 2000; Lau *et al.*, 2000a, b; Li *et al.*, 2000; Trievel *et al.*, 2000; Yamauchi *et al.*, 2000; Vo and Goodman, 2001; Lang and Hearing, 2003; Patel *et al.*, 2004). A number of transcriptional factors associate with p300/CBP, originally known as the global co-activator, and with PCAF and GCN5. Recruitment of these histone acetylases is thought to alter chromatin structures, and is required as an integral part of transcriptional activation. As a result of interaction with histone acetylases, certain transcription factors become acetylated themselves, which often results in enhanced transcriptional activity (Sterner and Berger, 2000). We have previously reported that the

Correspondence: Dr A Masumi, Department of Safety Research on Blood and Biological Products, National Institute of Infectious Diseases, 4-7-1, Gakuen, Musashimurayama-shi, Tokyo 208-0011, Japan. E-mail: amasumi@nih.go.jp
Received 30 June 2005; revised 22 February 2006; accepted 27 February 2006; published online 3 April 2006

transfection of PCAF-enhanced IRF-2-dependent *H4* promoter activity in NIH3T3 cells, (Masumi *et al.*, 1999) and that IRF-2 was acetylated by p300 and PCAF *in vivo* and *in vitro* (Masumi and Ozato, 2001), providing the first example of acetylation in the IRF family. Since then, additional IRF members IRF-3 and IRF-7, have been shown to be acetylated by p300 and PCAF, respectively, *in vivo* and *in vitro* (Caillaud *et al.*, 2002; Suhara *et al.*, 2002). Acetylation of IRF-2 leads to inhibition of histone acetylation by p300 *in vitro*, suggesting a possible mechanism for transcriptional repression by IRF-2 in U937 cells (Masumi and Ozato, 2001). In contrast, we demonstrated that acetylation of IRF-2 regulates cell growth by activation of the *H4* promoter (Masumi *et al.*, 2003). In NIH3T3 cells, IRF-2 associates with endogenous p300 and becomes acetylated, binds to an ISRE site, and activates *H4* promoter activity. Thus, we demonstrated that IRF-2 acts as repressor and activator through its acetylation. In this paper, which aimed to identify the protein that associates with acetylated IRF-2, we performed pull-down assay by using tagged a IRF-2 expression system and showed that IRF-2, acetylated by PCAF, recruits nucleolin and activates transcription. Nucleolin is reported to be a ubiquitously expressed multifunctional protein involved in ribosomal biogenesis and the regulation of nucleolar translocation of ribosomal proteins (Ginisty *et al.*, 1992; Srivastava and Pollard, 1999). Our results reveal a new function for nucleolin as an IRF-2-interacting partner and transcriptional activator.

Results

Exogenous p300/CBP-associated factor acetylates interferon regulatory factor-2 in 293T cells

We have demonstrated previously that IRF-2 acts as a transcriptional activator upon acetylation (Masumi *et al.*, 2003). To investigate IRF-2 acetylation by histone acetylases *in vivo*, flag-PCAF and flag-p300 were transfected into 293T cells with flag-IRF-2. Cells were labeled with ^{14}C-acetate 1 h before harvesting and a M2-agarose pull-down assay was performed (Figure 1). Western blot analysis of the immunoprecipitates using anti-flag M2 agarose indicated that these plasmid were expressed in 293T cells (Figure 1c). Western blot analysis of the immunoprecipitates using anti-flag M2 agarose showed that acetylation of flag-IRF-2 was enhanced by co-transfection with PCAF, and to a slightly lesser extent, by p300 (Figure 1a). The results from the incorporation of ^{14}C-acetate into p300, PCAF and IRF-2 in M2-agarose precipitates was in accordance with those seen with Western blotting (Figure 1b). The patterns of Western blotting with anti-acetyllysine antibody and the incorporation of ^{14}C-acetate in whole cell lysate transfected with any plasmid were almost similar between each lane (Figure 1a right and b right). To confirm that PCAFhistone acetyl transferase (HAT) acetylates IRF-2 in 293T cells, flag-PCAF and flag-PCAFΔHAT were transfected into 293T cells with flag-IRF-2. The pattern of Western blotting

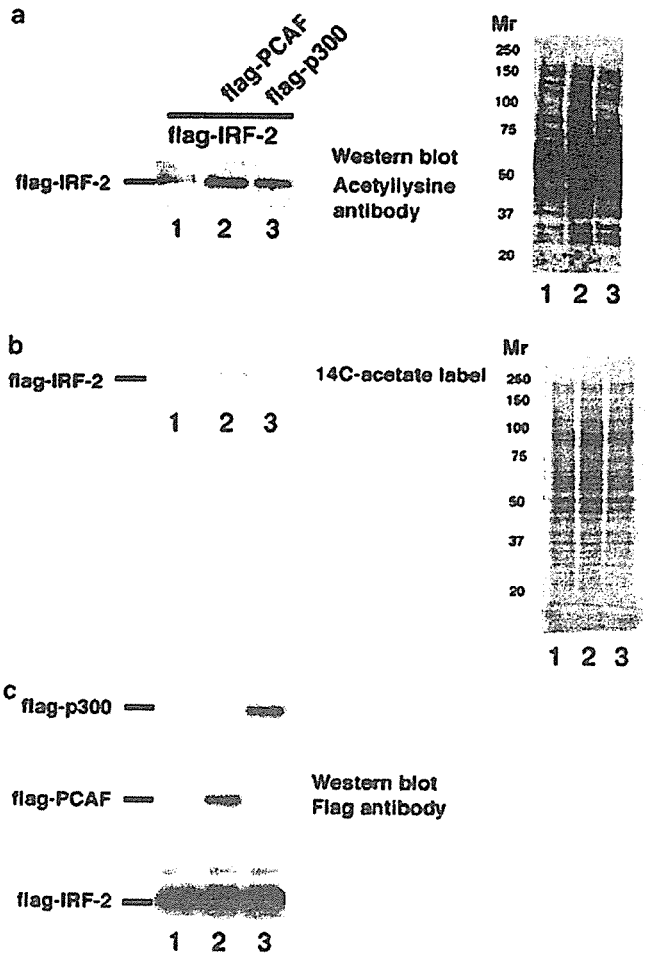

Figure 1 Interferon regulatory factor-2 (IRF-2) is acetylated by p300/CBP-associated factor (PCAF) and p300 in 293T cells. (**a**) 293T cells were transfected with flag-IRF-2 (1 μg) (lanes 1–3), together with flag-PCAF (1 μg) (lane 2) and flag-p300 (1 μg) (lane 3) plasmids. Of ^{14}C-acetate, 20 μCi were added 1 h before preparation of the cell lysate. Cell lysates from 293T cells were incubated with M2-agarose, and then the flag-peptide elution fraction was electrophoresed on SDS–10% PAGE and immunoblotted using an anti-acetyl lysine antibody (left). Whole lysate was electrophoresed on SDS–10% PAGE and immunoblotted with anti-acetyl lysine antibody (right) (**b**) Immunoblotted membranes from M2-agarose precipitates (left) and whole lysate (right) were reused for Image analysis using a Fuji BAS 2500 to visualize the ^{14}C-incorporated protein. (**c**) Anti-flag M2 agarose precipitates from 293T transfected cells transfected with above plasmids were electrophoresed on SDS–10% PAGE and immunoblotted with an anti-flag antibody.

for whole cell lysates did not significantly affect the results (Figure 2b). Western blot analysis of the immunoprecipitates using anti-flag M2 agarose indicated that these protein were expressed in 293T cells (Figure 2a bottom). An M2-agarose pull-down assay showed that compared to the control vector, the acetylation level of IRF-2 was increased by transfection of full-length PCAF, but not by PCAF lacking HAT activity (Figure 2a top). We detected PCAF autoacetylation as described earlier (Santos-Rosa *et al.*, 2003). These results indicate that IRF-2 acetylation is enhanced by PCAFHAT *in vivo*.

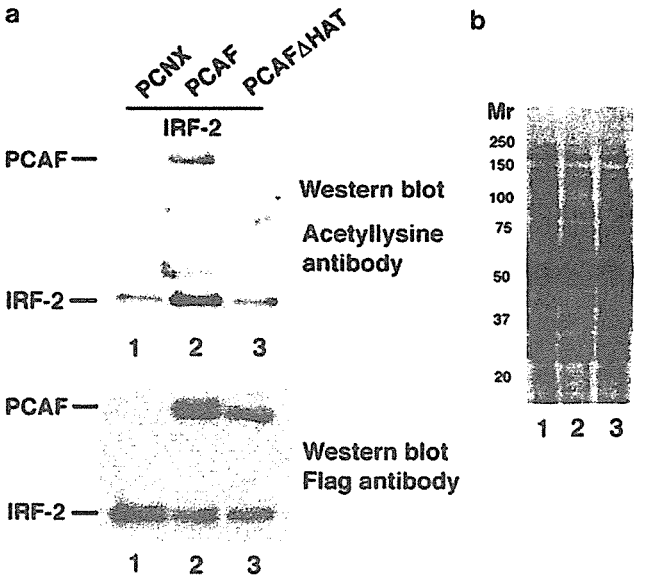

Figure 2 Western blot analysis of 293T cells transfected with interferon regulatory factor-2 (IRF-2) and p300/CBP-associated factor (PCAF). (**a**) 293T cells were transfected with PCNX control vector (lane 1), flag-PCAF (lane 2) and flag-PCAFΔhistone acetyl transferase (HAT) (lane 3) with flag-IRF-2. An M2-agarose-purified fraction from cell lysate was separated on SDS–10% PAGE and immunoblotted with an anti-acetyllysine (upper panel) or anti-flag antibody (bottom panel). (**b**) Whole cell lysates from transfected 293T cells were electrophoresed and immunoblotted with an anti-acetyllysine antibody. Full-length PCAF was auto-acetylated as shown in lane 2.

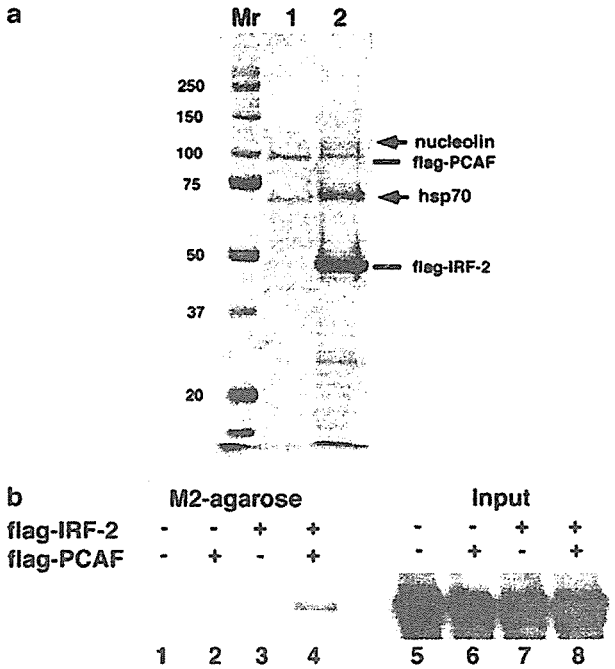

Figure 3 Coomasie blue staining pattern of the proteins co-precipitated with flag-interferon regulatory factor-2 (IRF-2). (**a**) 293T cells were transfected with 5 μg flag-p300/CBP-associated factor (PCAF) (lane1) alone and 5 μg flag-IRF-2 together with 5 μg flag-PCAF (lane 2). Whole cells were lyzed in a buffer B and incubated with M2-agarose, and then the flag-peptide-eluted fraction was separated on SDS–10% PAGE and the gel was stained with Coomasie brilliant blue. The two bands indicated with arrows were cut and trypsinized, and then liquid chromatography–mass spectrometry/mass spectrometry (LC–MS/MS) analysis was performed. Nucleolin was included in the upper band and the hsp70 family was included in the lower band. (**b**) 293T cells were transfected with control vector (lane 1), flag-PCAF (lane 2), flag-IRF-2 (lane 3), and flag-IRF-2 and flag-PCAF (lane 4) as described in (**a**). Cell lysates from 293T cells were incubated with M2-agarose, and then the flag-peptide elution fraction was prepared. Whole cells (right) and M2-agarose precipitates (left) were immunoblotted with anti-nucleolin antibody.

Interferon regulatory factor-2 recruits nucleolin in the presence of p300/CBP-associated factor

Our previous report suggested that it is the involvement of cellular proteins associated with acetylated IRF-2, which results in its transcriptional regulation (Masumi *et al*., 2003). To identify those proteins that associate with acetylated IRF-2, we performed an M2-agarose pull-down assay using 293T cells transfected with flag-IRF-2 and flag-PCAF. An M2-agarose-purified fraction was subjected to sodium dodecyl sulfate (SDS)–10% polyacrylamide gel electrophoresis (PAGE) and stained with Coomasie brilliant blue (Figure 3a). As shown in Figure 3a, proteins of approximately 110 and 70 kDa were observed in the immunoprecipitate from cells transfected with both flag-IRF-2 and flag-PCAF, but not in the immunoprecipitate from cells transfected with flag-PCAF alone. To identify these proteins, the bands were cut from the acrylamide gel, digested by trypsin and analysed by liquid chromatography–mass spectrometry/mass spectrometry (LC–MS/MS). Mass spectrometric analysis revealed that nucleolin was included in the 110-kDa band and that the heat shock protein 70 family was included in the 70 kDa band. As the heat shock protein 70 family is also included in the band in the PCAF-only transfected cells (Figure 3a, lane 1), we focused on nucleolin in this study. In Figure 3b, we investigated the nucleolin recruitment to IRF-2 using Western blotting. 293T cells were transfected with flag-IRF-2 in the presence or absence of flag-PCAF, and then cell lysate was incubated with anti-flag M2-agarose. The flag-peptide-eluted fraction was immunoblotted with anti-nucleolin antibody. Nucleolin expression level was not altered in any plasmid-transfected 293T cells, and nucleolin was detected most clearly in the flag-peptide-eluted fraction from cells transfected with both flag-IRF-2 and flag-PCAF (Figure 3b).

We investigated whether the histone acetylase activity of PCAF was required to recruit nucleolin to IRF-2. Flag-IRF-2 was cotransfected with flag-PCAF or flag-PCAFΔHAT into 293T cells and precipitated with M2-agarose, then analysed for the amount of recruited nucleolin by Western blotting. There was no difference of the amount of nucleolin in the lysate of 293T cells transfected with any cDNA (Figure 4a). Nucleolin was clearly identified in the affinity-purified complex from IRF-2/PCAF-transfected cells, but not in the precipitates from IRF-2/PCAFΔHAT-, IRF-2 alone-, or PCAF alone-transfected cells (Figure 4a), consistent with the

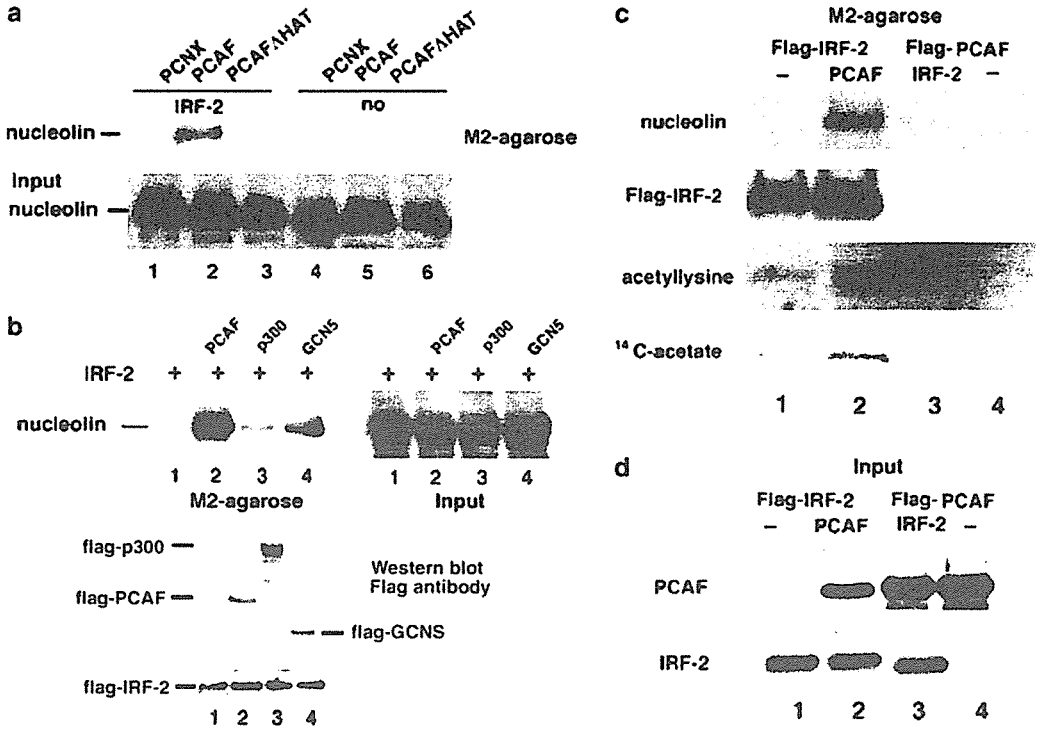

Figure 4 Nucleolin is involved in an interferon regulatory factor-2 (IRF-2)-binding complex. (**a**) Cell lysates from 293T cells transfected with PCNX (lanes 1 and 4), flag-p300/CBP-associated factor (PCAF) (lanes 2 and 5) and flag-PCAFΔhistone acetyl transferase (HAT) (lanes 3 and 6), flag-IRF-2 (lanes 1–3) were incubated with M2-agarose and the flag-peptide-eluted fraction was separated on a SDS–10% PAGE and immunoblotted with anti-nucleolin antibody (upper panel). Whole cell lysates from transfected 293T cells were separated on SDS–10%PAGE and immunoblotted with an anti-nucleolin antibody (bottom panel). (**b**) 293T cells were transfected with PCNX empty vector (lane 1), flag-PCAF (lane 2), flag-p300 (lane 3) and flag-GCN5 (lane 4) in the presence of flag-IRF-2. Cell lysate was incubated with M2-agarose and the flag-peptide-eluted fraction was separated on a SDS–10% PAGE and immunoblotted with anti-nucleolin antibody (upper left panel). Whole cell lysates from transfected 293T cells were separated on SDS–10%PAGE and immunoblotted with an anti-nucleolin antibody (upper right panel). Anti-flag M2-agarose precipitates from transfected 293T cells were immunoblotted with anti-flag antibody (bottom panel). (**c**) Acetylated IRF-2 preferentially recruits nucleolin in 293T cells. Flag-IRF-2 was transfected into 293T cells in the absence or presence of PCAF (without tag) (lanes 1 and 2) or flag-PCAF was transfected with or without IRF-2 (without tag) (lanes 3 and 4). ^{14}C-acetate was added to the 293T culture 1 h before harvesting. Cell lysates from 293T cells were incubated with M2-agarose and the flag-peptide fraction was electrophoresed and immunoblotted with anti-nucleolin, anti-flag, anti-acetyllysine antibodies. The membrane was reused for analysis with a BAS 2500 image analyzer to visualize ^{14}C-labeled protein. (**d**) Western blot analysis of PCAF and IRF-2 for whole 293T cells transfected with flag-IRF-2 (lanes 1 and 2), flag-PCAF (lanes 3 and 4), IRF-2 (lane 3) and PCAF (lane 2) was performed.

results of Figure 3b. To test whether IRF-2 recruits nucleolin in the presence of other histone acetylases, the same amount of p300 and GCN5 was transfected into 293T cells with IRF-2. As shown in Figure 4b, transfection of flag-p300 and flag-GCN5 also induced nucleolin recruitment to flag-IRF-2, although p300 recruited nucleolin to a much lesser extent compared to other histone acetylases. For comparative nucleolin recruitment to IRF-2, greater amounts of p300 may be required because of its larger molecular size. Nucleolin is not detected in the flag-peptide-eluted fraction from cell lysate transfected with only flag-IRF-2 although IRF-2 is acetylated at basal level in the absence of exogenous PCAF in 293T cells (Figures 1–4). Detectable basal acetylation level of IRF-2 does not have enough binding affinity with nucleolin in 293T cells.

To further investigate these results, PCAF without a flag-tag was transfected with flag-IRF-2 into 293T cells and then an M2-agarose pull-down assay was performed. Nucleolin was recruited more potently to affinity-purified precipitates of both flag-IRF-2 and PCAF-transfected cells than that of the cells transfected with flag-IRF-2 alone (Figure 4c). This result is similar to that was shown in Figure 4a. In addition, we detected an increase in IRF-2 acetylation in PCAF-transfected cells, consistent with the results in Figure 2. In contrast, when flag-PCAF was cotransfected with IRF-2 (without the flag-tag) into 293T cells, nucleolin was hardly detected in the anti-flag M2-agarose precipitates (Figure 4c).

We investigated whether an increased amount of PCAF transfection led to an increase in the recruitment of nucleolin to IRF-2. Differing amounts of PCAF was transfected into 293T cells with flag-tag IRF-2 and cell lysate was incubated with anti-flag M2 agarose, and the flag-peptide-eluted fraction was then immunoblotted with anti-acetyllysine, anti-nucleolin antibodies. Acetylation of IRF-2 and nucleolin recruitment increased parallel to amount of PCAF in 293T cells (Figure 5).

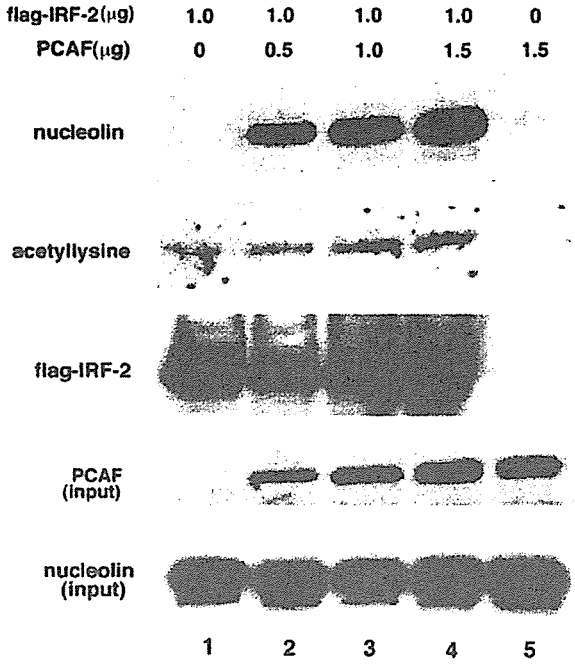

Figure 5 Interferon regulatory factor-2 (IRF-2) associates nucleolin in the presence of p300/CBP-associated factor (PCAF). 293T cells were transfected with several indicated amount of PCAF (lanes 1–5) and flag-IRF-2 (1 μg) (lanes 1–4). Cell lysate were incubated with anti-flag M2 agarose and flag-peptide eluted fraction were immunoblotted with anti-nucleolin, anti-acetyllysine and anti-flag antibodies. Whole cell lysate of transfected cells were immunoblot with anti-PCAF and anti-nucleolin antibodies.

We examined the localization of IRF-2 and nucleolin. HeLa cells transfected with flag-IRF-2 or a mutant flag-IRF-2K75R partially defective in acetylation (Masumi *et al*, 2003) with or without PCAF were fixed with paraformaldehyde and immunostained with an anti-flag antibody conjugated to cy3, and then an anti-nucleolin antibody linked with fluorescein isothiocyanate (FITC). Immunostained cells were visualized by laser scanning confocal microscopy. As shown in Figure 6a, there was no significant difference between wild-type IRF-2 and IRF-2K75R mutant-transfected HeLa cells, with nucleolin localized mainly in the nucleolus and to a lesser extent in the nucleus. Although IRF-2 localized predominantly in the nucleus, some was also localized in nucleolus. We observed that IRF-2 colocalized with nucleolin in a peri-nucleolar location. p300/CBP-associated factor transfection with both wild-type IRF-2 and K75R mutant did not change the colocalization of IRF-2 and nucleolin significantly.

To confirm if acetylatable IRF-2 recruits to nucleolin, a protein–protein interaction assay was performed using IRF-2 stably transfected cells. Cell lysates were prepared from HeLa and K562 cells stably transfected with flag-tagged wild-type IRF-2 or IRF-2K75R (Masumi *et al.*, 2003). Lysates were incubated with anti-flag M2-agarose, and the precipitates were subjected to Western blot analysis using an anti-nucleolin antibody. In both HeLa and K562 cells, appreciable amounts of PCAF and p300 were detected (data not shown). As shown in Figure 6b, nucleolin–IRF-2 interaction was observed in both HeLa and K562 cells that expressed wild-type IRF-2. However, in cells that expressed the K75RIRF-2 mutant (Masumi *et al.*, 2003), the nucleolin interaction was markedly diminished. These results suggest that IRF-2 is acetylated by histone acetylases such as PCAF and p300 in these cells, and that acetylated IRF-2 preferentially associates with nucleolin.

Nucleolin transactivates interferon regulatory factor-2-enhanced H4 promoter activity

Interferon regulatory factor-2 functions as an activator for the H4 gene promoter in NIH3T3 cells (Masumi *et al.*, 2003). To examine the functional role for nucleolin in IRF-2-dependent transcription, an *H4* gene reporter plasmid was transfected into NIH3T3 cells with IRF-2, PCAF and nucleolin. As shown in Figure 7a, transfection of nucleolin and PCAF both increased IRF-2-induced *H4* promoter activation. Co-transfection of nucleolin with PCAF further enhanced IRF-2-induced *H4* promoter activity (Figure 7a). In NIH3T3 cells, endogenous p300 may also induce IRF-2-dependent transactivation through acetylation, resulting in its interaction with nucleolin. In addition, co-transfection with HAT-deficient PCAF had no effect on nucleolin/IRF-2 activity. (Figure 7a). Co-transfection of the K75RIRF-2 mutant with PCAF/nucleolin resulted in a much lower activation of the *H4* promoter in NIH3T3 cells than with wild-type IRF-2 (Figure 7b). To examine nucleolin contribution to IRF-2-mediated *H4* promoter activation, we performed luciferase reporter assay using nucleolin small interfering RNA (siRNA). NIH3T3 cells were transfected with nucleolin siRNA to knock-down endogenous nucleolin and then transfected with IRF-2, PCAF with *H4* promoter-conjugated luciferase reporter. Compared to the control siRNA transfection, nucleolin siRNA transfection reduced the endogenous nucleolin protein in NIH3T3 cells (Figure 7d) and downregulated the IRF-2/PCAF-mediated *H4* promoter activation (Figure 7c). These results confirm that nucleolin contributes to IRF-2/PCAF-mediated transcriptional activation in NIH3T3 cells.

We have shown previously that acetylation of IRF-2 is related to cell growth (Masumi *et al.*, 2003) and have therefore investigated whether IRF-2 is associated with nucleolin in growing NIH3T3 cells. For confocal analysis, we detected that IRF-2 and nucleolin were localized in nuclei and nucleoli in both growing and growth-arrested NIH3T3 cells. There was no significant difference between either type of NIH3T3 cell (Figure 8a). We performed a DNA affinity binding assay with biotinylated *H4* promoter oligonucleotides that had been conjugated to magnetic beads. Nuclear extracts from growing and growth-arrested cells were incubated with the beads-conjugated *H4* promoter DNA. Interferon regulatory factor-2 was detected in an eluted fraction from beads incubated with growing cell nuclear extract as reported earlier (Figure 8b) (Masumi *et al.*, 2003). We found that while a similar level of nucleolin was detected in both growing and growth-arrested cells, H4 promoter DNA was bound to

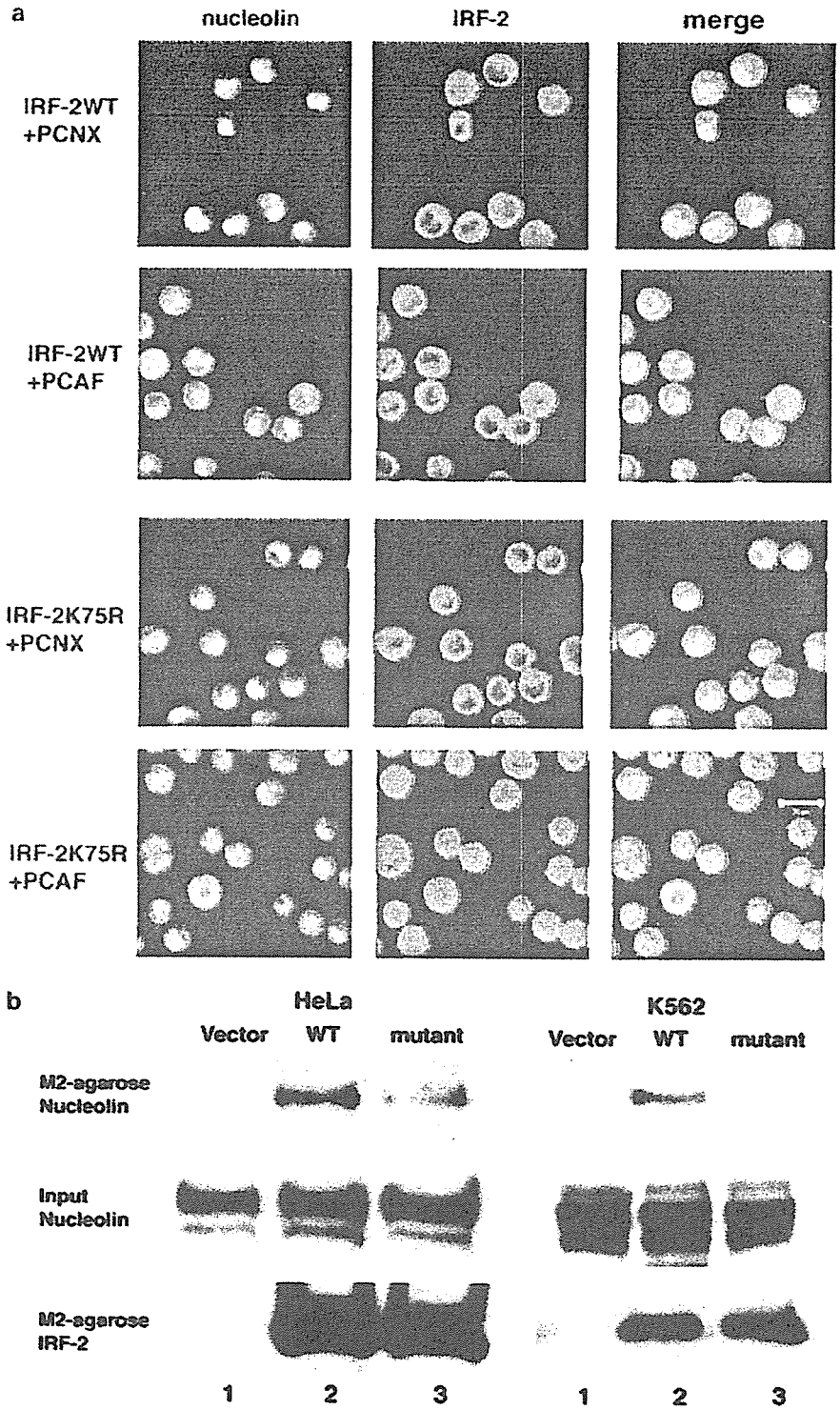

Figure 6 Interferon regulatory factor-2 (IRF-2) colocalizes and associates with nucleolin. (**a**) Laser scanning confocal microscopy was carried out on HeLa cells transiently transfected with flag-IRF-2 and flag-IRF-2K75R with or without p300/CBP-associated factor (PCAF). The cells were fixed with paraformaldehyde 24 h after transfection and lysed with 0.2% TritonX-100 for 10 min. Then, cells were immunocytostained with a anti-flag conjugated to Cy3 (red fluorescence) antibody for 24 h, following which, washed cells were immunostained with anti-nucleolin linked with fluorescein isothiocyanate (FITC) (green fluorescence) for 24 h. These washed cells were covered with glycerol and examined by laser scanning confocal microscopy. Colocalization of proteins results in a merging of red and green fluorescence to produce a yellow image. (**b**) Cell lysate from HeLa (left) and K562 (right) cells stably transfected with an empty vector (lane 1), flag-IRF-2 (lane 2) and flag-IRF-2K75R mutant (lane 3) were incubated with anti-flag M2-agarose and flag-peptide-eluted fractions were separated on SDS–10% PAGE and immunoblotted with anti-nucleolin (top) and anti-IRF-2 (bottom) antibodies. Whole cell lysates were separated on SDS–10% PAGE and immunoblotted with an anti-nucleolin antibody (middle).

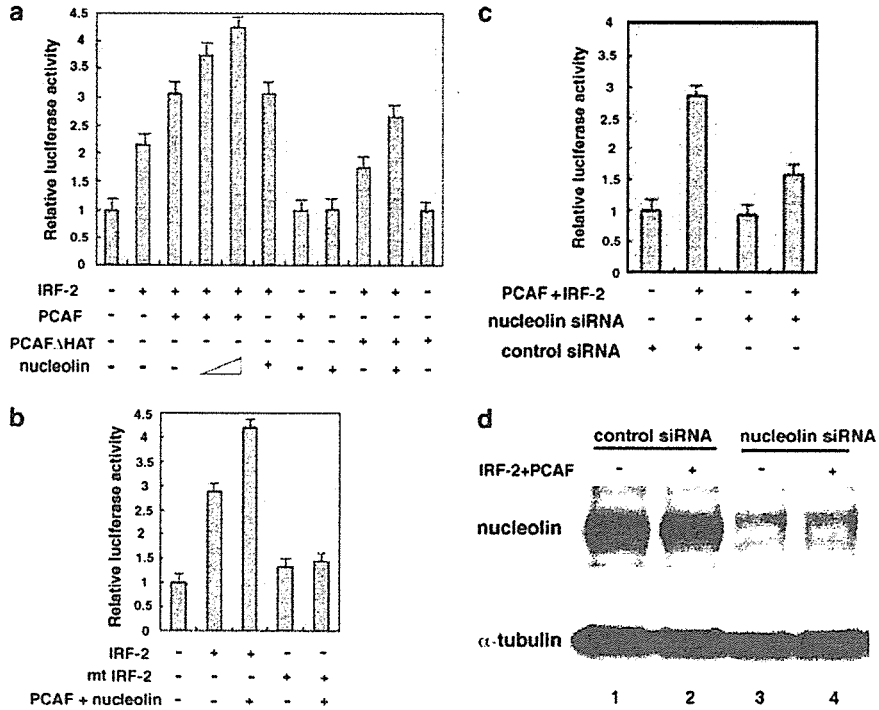

Figure 7 Nucleolin activates interferon regulatory factor-2 (IRF-2)-dependent *H4* promoter activity. (**a**) *H4* promoter reporter (400 ng), nucleolin (100 and 200 ng), p300/CBP-associated factor (PCAF)PCNX (100 and 200 ng) and PCAFΔhistone acetyl transferase (HAT)PCNX (200 ng) were transfected with IRF-2pcDNA3.1 (20 ng) into NIH3T3 cells. Luciferase activity was analysed 48 h after transfection. (**b**) Wild-type IRF-2 or mutant IRF-2 (IRF-2K75R) was transfected with nucleolin/PCAF with the *H4* promoter reporter as described in (**a**). Luciferase activity was analysed 48 h after transfection. The mean ± s.d. from three separate experiments were calculated after normalization with TK Renilla activity. (**c**) Nucleolin small interfering RNA (siRNA) abrogates IRF-2/PCAF-induced *H4* promoter activation. Nucleolin siRNA was transfected into NIH3T3 cells and then PCAFPCNX and IRF-2pcDNA3.1 were transfected into NIH3T3 cells with *H4* promoter reporter. At 24 h after transfection of plasmids, luciferase activity was analysed. (**d**) Immunoblot analysis of NIH3T3 cell lysate transfected with nucleolin siRNA and plasmids as described in (**c**) using anti-nucleolin and anti-α-tubulin antibodies.

the nucleolin from growing cells only (Figure 8b). These finding are consistent with previous results, which support that the interaction of nucleolin and acetylated IRF-2 in growing cells mediate *H4* gene promoter activity (Masumi *et al.*, 2003).

From these results, it appears that the acetylation of IRF-2 rather than the change of colocalization of both factors is important for the interaction of IRF-2 and nucleolin in growing NIH3T3 cells. To confirm the association of nucleolin with IRF-2 on the *H4* promoter, chromatin immunoprecipitation analysis was performed. Chromatin was isolated from NIH3T3 cells transfected with PCAFPCNX and immunoprecipitated with anti-IRF-2 and anti-nucleolin and anti-PCAF antibodies. Immunoprecipitates were performed with polymerase chain reaction (PCR) using *H4* promoter primer as described earlier (Masumi *et al.*, 2003). As shown in Figure 8c, PCAF transfection slightly enhance the PCAF binding to *H4* promoter, however, a greater amount of nucleolin was bound to the *H4* promoter in the PCAF-transfected cells compared to control cells. In addition, a greater amount of IRF-2 was also bound to the *H4* promoter in PCAF-transfected cells compared to non-transfected cells. From these results it appears that, in NIH3T3 cells, IRF-2 and nucleolin bound the *H4* promoter more tightly following transfection with exogenous PCAF. We conclude that nucleolin binds to acetylated IRF-2 and IRF-2/PCAF/nucleolin complexes in turn stimulate the activation of gene transcription, which drives cell growth (Figure 9).

Discussion

In this study, we have demonstrated that nucleolin acts as a positive modulator of IRF-2-dependent transcriptional activation through an association with IRF-2. Nucleolin is one of the most abundant nucleolar proteins in rapidly growing eukaryotic cells. It is multifunctional and thought to be involved in many cellular processes, including ribosome biogenesis, the processing of ribosomal RNA, mRNA stability, transcriptional regulation and cell proliferation, and it is also a downstream target of several signal transduction pathways (Ginisty *et al.*, 1992; Srivastava and Pollard, 1999). Nucleolin has been shown by proteomic analysis to associate with various proteins, such as B23, Ku80, eIF2a and the RNA binding proteins (RNP) complex (Yanagida *et al.*, 2001). Ying *et al.* (2000) reported that the interaction of nucleolin with Myb downregulated Myb transcriptional activity. Recently, Grinstein *et al.*

(2002) reported that nucleolin is a key activator of the HPV18 oncogene transcription involved in chromatin structure regulation and thus identified nuclelolin as a cellular protein with oncogenic potential. From our study we can conclude that for *H4* gene regulation by IRF-2, nucleolin acts as an oncogenic activator via

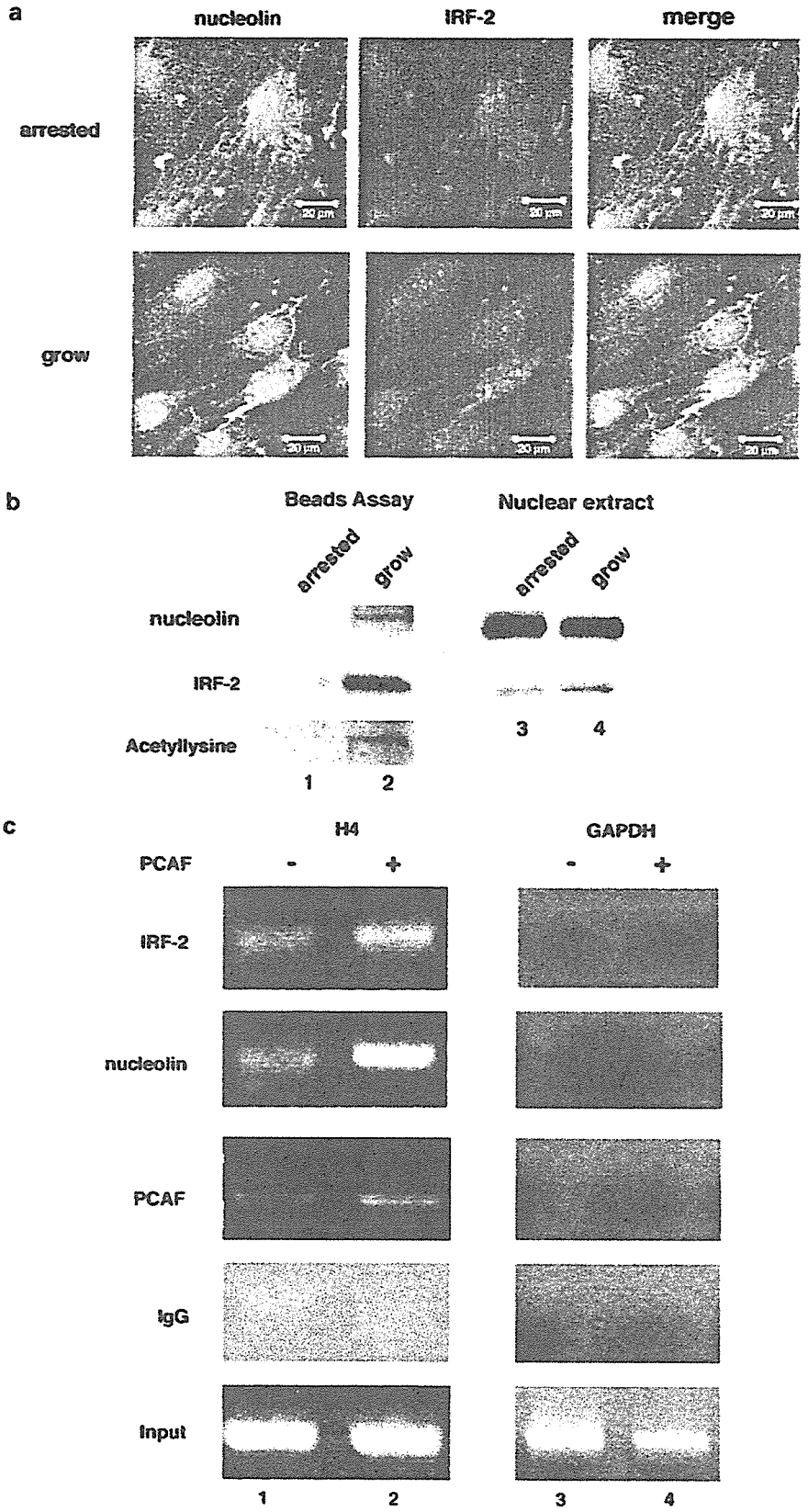

transcriptional activation, suggesting an involvement in cell growth regulation.

Previously, we demonstrated in NIH3T3 cells that lysine residues 75 and 78 in the IRF-2 DNA-binding domain are the major acetylation sites and that the IRF-2K75R mutant showed reduced *H4* promoter activity. As reported in our previous paper, p300 acts as the main acetylase for IRF-2 in NIH3T3 cells because the level of PCAF expression is so very low. However, exogenous PCAF transfection induced IRF-2-dependent transcriptional activation (Masumi *et al.*, 1999), and exogenous PCAF might induce IRF-2 acetylation in NIH3T3 cells. We also found that transfection with another histone acetylase GCN5 induced IRF-2 acetylation (data not shown) and nucleolin-IRF-2 interaction in 293T cells. We previously concluded that in NIH3T3 cells acetylated IRF-2 binds to the *H4* promoter with p300 to regulate the H4 gene (Masumi *et al.*, 2003). However, in cells with a high amount of PCAF or GCN5, IRF-2 may be acetylated by both histone acetyltransferases, as well as p300, recruit nucleolin and thus regulate specific promoters. In the *H4* promoter assay, we demonstrated that PCAF acetyltransferase activity was required for efficient activation of transcription mediated by IRF-2/nucleolin. Interferon regulatory factor-2K75R mutant partially defective acetylation reduces the activation of the *H4* promoter in the presence of PCAF/nucleolin, consistent with the results of the poor association of IRF-2K75R with nucleolin in stable transfectants.

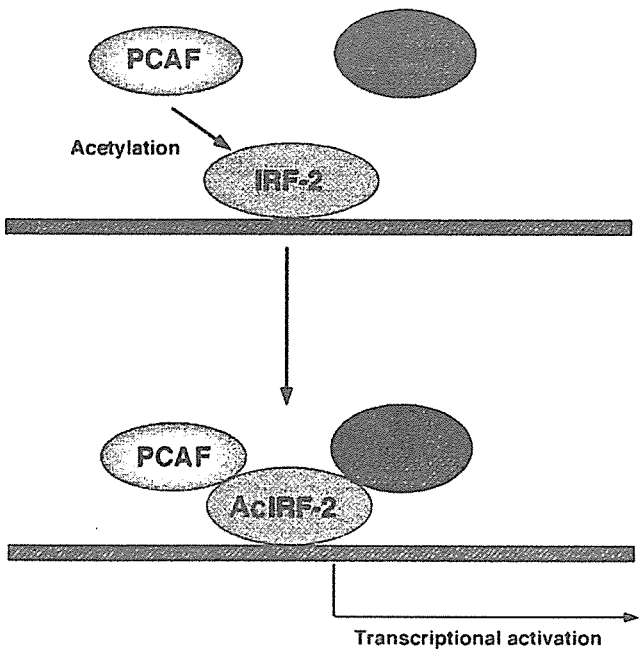

Figure 9 Schematic model of the interferon regulatory factor-2 (IRF-2)-binding complex for its transcriptional regulation. p300/CBP-associated factor (PCAF) acetylates IRF-2, and acetylated IRF-2 associates with endogenous nucleolin together with PCAF. IRF-2/nucleolin/PCAF transactivates the IRF-2-specific promoter.

We observed that in HeLa cells, IRF-2 colocalized with nucleolin in the peri-nucleolar region. Nucleolin has been reported to colocalize with p53 in a stress-dependent manner; it mobilizes between nucleoli, nuclei and the cytosol depending on the level of stress (Klibanov *et al.*, 2001; Daniely *et al.*, 2002). This mobilization depends on the cell condition, such as during various stage of growth or differentiation. In our confocal experiment, PCAF expression did not change the localization of either IRF-2 or nucleolin in HeLa cells. In growing and growth-arrested NIH3T3 cells, similar colocalization of nucleolin and IRF-2 is observed. p300/CBP-associated factor-mediated acetylation induces nucleolin-binding affinity to IRF-2 rather than colocalization of both factors.

Treatment with trichostatin A, a typical histone deacetylase inhibitor, enhanced both expression and acetylation of IRF-2 in IRF-2-stably transfected HeLa cells, but the association of IRF-2 with nucleolin was comparable between trichostatin A-treated and untreated HeLa cells (data not shown). Trichostatin A may affect other acetylatable transcription factors, which compete with IRF-2/nucleolin interaction. Alternatively, interaction of PCAF and p300 with IRF-2 may be required for the association of nucleolin and acetylated IRF-2. In fact, as IRF-2 binds PCAF or p300 *in vitro* and *in vivo* as reported earlier (Masumi *et al.*, 2003), acetylated IRF-2 may associate with nucleolin together with PCAF or p300. However, the nucleolin recruitment in anti-flag M2 agarose precipitate from flag-tagged PCAF-transfected cells was difficult to detect. From these results it can be concluded that nucleolin binds to IRF-2 directly, but not to PCAF. Acetylated IRF-2 could be detected at the basal level in

Figure 8 Nucleolin binds *H4* promoter. (**a**) Laser scanning confocal microscopy was carried out on NIH3T3 cells. Growing or growth-arrested NIH3T3 cells were fixed with paraformaldehyde 24 h after transfection and lysed with 0.2% TritonX-100 for 10 min. Cells were then immunocytostained with a goat anti-interferon regulatory factor-2 (IRF-2) antibody at 4°C overnight and then immunostained with anti-goat second antibody conjugated to Alexa 488 for 2 h (green fluorescence). Following this, washed cells were immunostained with rabbit anti-nucleolin antibody and then anti-rabbit second antibody linked with Alexa 594 (red fluorescence) for 2 h. Washed cells were covered with glycerol and examined by Laser scanning confocal microscopy. Colocalization of proteins results in a merging of red and green fluorescence to produce a yellow image. (**b**) Nucleolin interacts with IRF-2 in growing NIH3T3 cells. Nuclear extracts were prepared from growth-arrested (lanes 1 and 3) and growing NIH3T3 cells (lanes 2 and 4), and incubated with magnetic beads conjugated to *H4* promoter. Bound materials (lanes 1 and 2) and whole nuclear extract (lanes 3 and 4) were analysed by immunoblot assay using anti-nucleolin, anti-IRF-2 and anti-acetyllysine antibodies. (**c**) NIH3T3 cells were transfected with p300/CBP-associated factor (PCAF) and crosslinked with 1% formaldehyde, chromatin was isolated as described under 'Materials and methods' and a chromatin immunoprecipitation assay of the *H4* promoter and glyceraldehyde-3-phosphate dehydrogenase (GAPDH) using anti-IRF-2, anti-nucleolin, anti-PCAF and rabbit immunoglobulin G (IgG) was performed. Polymerase chain reaction (PCR) quantitation was carried out as indicated under 'Materials and methods.'

IRF-2-transfected 293T cells without transfection of PCAF (Figures 1–5). However, we could not detect significant nucleolin recruitment to flag-IRF-2 without transfection of PCAF. p300/CBP-associated factor transfection led to a great extent of nucleolin recruitment instead of slight increase of acetylation of IRF-2, although increasing the extent of PCAF transfection increased nucleolin recruitment and was consistent with IRF-2 acetylation (Figure 5). Acetylated IRF-2 may change its conformation and nucleolin may prefer to bind to acetylated IRF-2. Nucleolin has many acid residues such as glutamic acid and asparagic acid (Lapeyre *et al.*, 1987). In contrast, IRF-2 has 18 lysine residues in DNA-binding domain (Masumi *et al*, 2003). We do not at present understand how they associate via their amino acids charge, but expect to be able to determine the binding form for both factors in the future. p300/CBP-associated factor transfection may not only enhance the acetylation but also the binding affinity of IRF-2 with nucleolin. According to the chromatin precipitation analysis, PCAF transfection enhanced nucleolin and IRF-2 binding to *H4* promoter, but PCAF binding to H4 promoter was enhanced only slightly by PCAF transfection. Exogenous PCAF may contribute to the acetylation of IRF-2 rather than an association with *H4* promoter.

As shown in Figure 4b, p300 transfection into cells induced much less amount of nucleolin recruitment to IRF-2 compared to PCAF transfection. Although PCAF appeared to be a slightly better IRF-2 acetylase, transfection of p300 also resulted in substantial acetylation of IRF-2 (Figure 1a). It is not clear why p300 only induced modest recruitment of nucleolin to IRF-2 (Figure 4b), despite fairly high level of IRF-2 acetylation. p300 may acetylate other proteins which compete with IRF-2 for binding to nucleolin. We are currently searching for other acetylated proteins that associate with nucleolin when PCAF or p300 is transfected.

It has been shown that p300 and PCAF interact with and acetylate HIV Tat on distinct lysine residues (Kiernan *et al.*, 1999; Ott *et al.*, 1999). The acetylation of the activator domain of Tat by PCAF and p300 has different biological functions for Tat, and both events increase the activation of transcription from the LTR (Ott *et al.*, 1999, 49). In addition, Chen *et al.* (2002) demonstrated that acetylation of RelA at distinct sites differentially regulates various biological functions of NF-κB. Martinez-Balbas *et al.* (2000) showed that acetylase PCAF, and to a lesser extent CBP and p300, can acetylate E2F1 *in vivo* and increase its DNA-binding ability and that the acetylation status of E2F1 is affected by the histone deacetylase associated with the RB–E2F1 complex. Thus, acetylation of transcription factors leads to changes in their biological activity in terms of DNA-binding affinity, transcriptional activity, interaction with other proteins, and intracellular protein stability (Bannister and Miska, 2000). In the case of IRF-2, we demonstrated that the same sites of IRF-2 were acetylated by PCAF and p300 and that acetylated IRF-2 bound to the promoter more efficiently than non-acetylated IRF-2 *in vivo* as shown earlier (Masumi *et al.*, 2003). Acetylated and non-acetylated IRF-2 appear to bind differently to cellular proteins. Acetylated IRF-2 binds to promoters more efficiently, probably by recruiting cellular factors, such as the nucleolin identified in this study.

Barlev *et al.* (2001) showed that acetylated p53 binds more tightly to the transcriptional cofactors transformation/transcription domain-associated protein (TRRAP) and CREB-binding protein than non-acetylated p53, although acetylated and non-acetylated p53 bind to the p21 promoter in the same manner. Levy *et al.* (2004) demonstrated that acetylated β-catenin associates preferentially with Tcf4 (T-cell factor/lymphoid enhancer factor) and that co-activaion of β-catenin/Tcf by p300 is mediated in part by acetylation of β-catenin. In our study, we have confirmed that PCAF-acetylated IRF-2 forms a complex with nucleolin. Histone acetylases such as PCAF and p300 mediate IRF-2-dependent transcriptional activation through nucleolin–IRF-2 interaction. Our findings provide the biological evidence for a transcriptional regulatory mechanism which is effected via protein acetylation.

Materials and methods

Cell culture and transfection

NIH 3T3 cells were grown in Dulbecco's-modified Eagle's medium (DMEM) (Sigma, St. Louis, MI, USA) with 10% calf serum (GIBCO BRL, Rockvile, MD, USA), penicillin (100 U/ml) and streptomycin (100 μg/ml) at 37°C in 5% CO_2 and 95% air. NIH 3T3 cells were transfected with H4 reporter using lipofectamine (Invitrogen, Carlsbad, CA, USA) as described earlier (Masumi *et al.*, 2003). For making growth-arrested NIH3T3 cells, DMEM containing 0.5% calf serum was added to growing NIH3T3 cells, and cells were cultured for 48 h. HeLa and 293T cells were grown in DMEM with 10% fetal calf serum (Sigma). 293T cells were then transfected with IRF-2pcDNA3.1, PCAFPCNX and p300pCI plasmids (Masumi *et al*, 1999; Masumi and Ozato, 2001) using Fugene 6 (Roche Biochemicals, Indianapolis, IN, USA). At 24–48 h after transfection, cells were lysed in a buffer B (Tris-HCl, pH 8.0, 0.1 mM ethylenediamine tetraacetic acid (EDTA), 100 mM NaCl, 0.1% NP-40), containing a protease inhibitor mix (Sigma). For some experiments, 20 μCi of ^{14}C-acetate (Amersham, Piscataway, NJ, USA) were added 1 h before preparation of the cell lysate. Cell lysates were used for an anti-flag M2-agarose pull-down assay. K562 cells were cultured in RPMI medium (Sigma) with 10% fetal calf serum. To produce stable transfectants, HeLa and K562 cells were transfected with IRF-2 or IRF-2K75R (Masumi *et al.*, 2003) using Fugene 6 (Roche Biochemicals) and cultured for 2 weeks in the presence of 400 μg/ml G418. G418-resistant cells were pooled and lysed for preparation of cell lysate. The nucleolin plasmid was a kind gift from Dr S Murakami (Hirano *et al.*, 2003).

Western blotting

Whole cell lysates were prepared in lysis buffer B, with the addition of a protease inhibitor cocktail (Sigma). The insoluble materials and whole cell lysates containing equal amounts of total proteins were suspended in an SDS sample buffer boiled, separated on SDS–10% PAGE, and transferred onto polyvinylidene difluoride membranes (Millipore, Bedford, MA, USA). The membranes were blocked with 5% non-fat dry milk

in a phosphate-buffered saline (PBS)-T buffer (PBS containing 0.5% Tween 20) for 1 h, incubated with anti-IRF-2 (Santa Cruz), anti-p300 (Santa Cruz), anti-acetyl lysine (New England Biology, Beverly, MA, USA) and anti-flag (Sigma) antibodies for 1 h, and washed in PBS-T. The antigen–antibody interaction was visualized by incubation in a chemiluminescent reagent (Perkin Elmer Co. Ltd) and exposure to X-ray film. Immunoblotted membranes were reused for Image analysis using a Fuji BAS 2500 (Fuji Film, Japan) to visualize ^{14}C-incorporated protein.

Affinity DNA-binding assay
The DNA affinity-binding assay was performed as described (Masumi *et al.*, 2003). Briefly, nuclear extracts (500 μg of protein) were incubated with magnetic beads conjugated to biotinylated oligonucleotide from the H4 gene. Bound materials were immunoblotted with anti-nucleolin antibody.

Chromatin immunoprecipitation
A total 1×10^7 NIH3T3 cells were crosslinked with 1% formaldehyde for 15 min at room temprature. Cells were washed with PBS and resuspended in 1 ml of lysis buffer (1% SDS, 10 mM EDTA, 50 mM Tris-HCl, pH 8.0) plus a protein inhibitor mixture (Sigma), incubated on ice for 10 min, and sonicated to an average size of 500 bp by an ultrasonic cell disruptor (Ultra 5 homogenizer, TAITEC). Aliquots (100 μl) of sonicated chromatin were diluted in 1 ml of buffer (1%Triton X-100, 2 mM EDTA, 150 mM NaCl, 20 mM Tris-HCl, pH 8) and precleared with 2 μg of sheared salmon sperm DNA and protein G-Sepharose (Invitrogen) for 2 h at 4°C. Immunoprecipitation was performed overnight at 4°C with anti-IRF-2, anti-nucleolin (Santa Cruz) anti-PCAF (UBI) and rabbit immunoglobulin G (IgG) (Sigma). A 50-μl aliquot protein G-Sepharose, and 2 μg of salmon sperm DNA were added to each immunoprecipitation and incubated for 1 h. Precipitates were washed as described earlier and samples were extracted twice with elution buffer (1%SDS, 0.1 M $NaHCO_3$), heated at 65°C to reverse crosslinks, and DNA fragments were purified with phenol/chloroform. A 5-μl aliquot from a total of 30 μl was used in the PCR as descried earlier (Masumi *et al.*, 2003).

Purification of interferon regulatory factor-2 precipitates and analysis of mass spectrometry
Cell lysates were prepared from 293T cells transfected with IRF-2 (flag-tag or no-tag) and PCAF (flag-tag or without tag) and incubated with 50–100 μl M2 agarose (Sigma) for 2 h with rotation. After washing with buffer B, bound proteins were eluted from M2 agarose by incubation for 5 min with 30 μl of the flag peptide (0.2 mg/ml) (Sigma) in the same buffer. Eluted protein was separated on SDS–PAGE and stained with Simply blue (Invitrogen). To identify the IRF-2-associated protein, a sliced band from the gel was digested with trypsin and peptides were analysed by LC–MS/MS using LCQ-Deca XP ion trap mass spectrometer (Thermo Electron Corp., Waltham, MA, USA).

M2-agarose pull-down assay
For the M2-agarose pull-down assay, cell lysates from the 293T transfectants were incubated with M2 agarose (Sigma) in buffer B and washed three times. Bound materials were eluted by a 0.2 mg/ml flag peptide (Sigma), resolved on SDS–12.5% PAGE, and detected by Western blotting.

Small interfering RNA experiments
NIH3T3 cells were seeded at density of 3×10^5 cells per ml onto 24-well plate. After 16 h, cells were transfected with 100 mM siRNA oligonucleotides by RNAiFect Transfection Reagent (QIAGEN, Hilden, Germany) and the siRNA-containing medium was removed after 24 h of transfection, and then IRF-2pcDNA3.1, PCAFPCNX with H4 promoter luciferase reporter were transfected into NIH3T3 cells by lipofectamine (Invitrogen). Luciferase activity was analysed 24 h after transfection with plasmids. The sequences of siRNAs used here were as follows: nucleolin, GCUUUAAAUUCCU-GUAAUATT, negative control, non-silencing Alexa Flour 488 Labeled Control siRNA (QIAGEN).

Confocal microscopy
For laser scanning focal microscopy experiments, HeLa cells were cultured in a 35 mm glass bottom dish (Matsunami Glass Ind. Ltd, Japan). At 24 h after transfection, the cells were fixed with paraformaldehyde and lysed with 0.2% TritonX-100 in order to maintain the integrity of the cellular structures. They were then stained with appropriate antibodies as follows: cells transfected with flag-IRF-2 were stained with an anti-flag M2-Cy3 (Sigma). Cells were subsequently stained with anti-nucleolin-linked FITC (Santa Cruz 'sc-8023') for 16 h. NIH3T3 cells were stained with an goat anti-IRF-2 antibody (Santa Cruz) for 16 h and then with an anti-goat second antibody linked to Alexa 488 (Molecular Probes Inc., Eugene, OR, USA) for 2 h. Cells were subsequently stained with rabbit anti-nucleolin antibody (Santa Cruz), and then anti-rabbit IgG-linked Alexa 594 (Molecular Probe Co. Ltd). Stained cells were washed with Tris-buffer saline and mounted on glass slides with a mounting medium (glycerol-PBS). Fluorescent images were collected on a Zeiss Axiovert 100 confocal microscope using a Zeiss $\times 40$ objective.

Acknowledgements

This work was supported by the Japan Society for Promotion of Sciences and the Ministry of Education, Science, Sports and Culture and the Japan Health Sciences International Foundation. We thank Dr Y Nakatani for providing plasmids, Dr K Sakai and Dr M Kasai for technical advices, Dr K Kamemura, Dr A Ito, Dr Y Murakami and Dr I Hamaguchi for useful discussions, and Dr A Fuse and Dr Y Uehera for general support.

References

Bannister AJ, Miska EA. (2000). *Cell Mol life Sci* **57**: 1184–1192.
Barlev N, Liu L, Chehab N, Mansfield K, Harris K, Halazonetis T *et al.* (2001). *Mol Cell* **8**: 1243–1254.
Benkirane M, Chun RF, Xiao H, Ogryzko VV, Howard BH, Nakatani Y *et al.* (1998). *J Biol Chem* **273**: 24898–24905.
Caillaud A, Prakash A, Smith E, Masumi A, Hovanessian A, Levy D *et al.* (2002). *J Biol Chem* **277**: 49417–49421.
Chen L-F, Mu Y, Greene WC. (2002). *EMBO J* **21**: 6539–6548.
Chow W, Fang J, Yee J. (2000). *J Immunol* **164**: 3512–3518.
Daniely Y, Dimitrova DD, Borowiec JA. (2002). *Mol Cell Biol* **22**: 6014–6022.